THE ASTROPHYSICAL JOURNAL, 220:75–97, 1978 February 15

PHOTOMETRIC STUDIES OF COMPOSITE STELLAR SYSTEMS. I. CO AND *JHK* OBSERVATIONS OF E AND S0 GALAXIES

JAY A. FROGEL,* S. E. PERSSON,† MARC AARONSON,‡ AND K. MATTHEWS§
Received 1977 March 8; accepted 1977 August 19

ABSTRACT

New multiaperture infrared photometric observations of the central regions of 51 early-type galaxies and of the integrated light of five globular clusters are presented. These data are compared with selected optical observations and with various model predictions. The main results of the work are: (1) the observed parameters for the brighter galaxies, particularly the CO index and the $V - K$ color, agree with the predictions of stellar synthesis models characterized by giant-dominated populations with $M/L_V < 10$; (2) the galaxian broad-band colors tend to redden with increasing luminosity and decreasing aperture size; (3) for the globular clusters, there is evidence that the integrated colors become redder with increasing metallicity; and (4) in bright galaxies the relative changes of $U - V$, $V - J$, and $J - K$ as functions of radius may differ from the relative changes as functions of luminosity at a fixed radius.

Subject headings: clusters: globular — galaxies: photometry — galaxies: stellar content — infrared: sources

I. INTRODUCTION

The composite nature of the integrated spectra of elliptical galaxies and the domination of the visible light by late-type giant stars have been known for nearly 30 years (e.g., Stebbins and Whitford 1948; Morgan and Mayall 1957; Code 1959; reviewed by Whitford 1976). Nevertheless, the lack of luminosity-sensitive indices, particularly in the red and infrared regions of the spectrum, has hindered attempts to build quantitative models of the stellar content of these galaxies. For example, one of the conclusions of a study by Faber (1972), based in part on the observations of Spinrad and Taylor (1971), was that the available optical data could not be used to uniquely determine the proportion of high- and low-luminosity red stars. The first broad-band infrared observations of galaxies (Johnson 1966*a*) showed that the 1.2–3.5 μm radiation is contributed mostly by stars cooler than those which dominate the visible light. However, M dwarfs and M giants have similar colors in the infrared, so that Johnson's data were not adequate to determine the relative contributions of the high- and low-luminosity populations.

Advances in the development of red- and infrared-sensitive detectors have finally permitted the accurate measurements of both luminosity- and temperature-sensitive indices in these spectral regions. Examples of such observations are those of the Ca II + TiO features by O'Connell (1974, 1976*a*, *b*), the 2.3 μm CO band by Baldwin *et al.* (1973), and Frogel *et al.* (1975*b*), and the 9910 Å Wing-Ford band by Whitford (1977). These data are necessary to model the stellar content of elliptical galaxies, and hence to estimate the evolutionary correction to q_0 in the redshift-magnitude diagram (Sandage 1961; Faber 1973*b*; Tinsley 1973, 1975; Tinsley and Gunn 1976; O'Connell 1976*b*).

In this paper we present new multiaperture observations of the strength of the CO feature in 51 elliptical and lenticular galaxies. Together with these measurements, we have also obtained magnitudes in the 1.2 μm, 1.6 μm, and 2.2 μm photometric bands (J, H, and K) for the same galaxies. These data are combined with U and V observations from the literature to examine variations in the relationships between optical and infrared colors from galaxy to galaxy and within individual galaxies. In § II, the photometric system, observational procedures, and data reduction are described in some detail. The results of the observations are presented in §§ III and IV. In §§ V and VI, the results are compared with published stellar synthesis models and with other photometric studies of galaxies. Our conclusions are summarized in § VII. The system of standard magnitudes and colors, and mean photometric relationships for a selection of red-giant and dwarf stars, are presented in the Appendix.

Paper II of this series (Aaronson, Frogel, and Persson 1978) presents observations of the 2.0 μm H_2O absorption band (Baldwin, Frogel, and Persson 1973), which impose additional constraints on the coolest stellar component of the galaxies under investigation. Paper III (Persson, Frogel, and Aaronson 1978) presents new multiaperture *UBVR* and *JHK* data for

* Cerro Tololo Inter-American Observatory and Kitt Peak National Observatory, which are operated by the Association of Universities for Research in Astronomy, Inc., under contract with the National Science Foundation. Guest Investigator at the Hale Observatories.

† Hale Observatories, Carnegie Institution of Washington, California Institute of Technology.

‡ Smithsonian Predoctoral Fellow, Center for Astrophysics, Harvard College Observatory and Smithsonian Astrophysical Observatory. Guest Investigator at Kitt Peak National Observatory and Las Campanas Observatory, Carnegie Institution of Washington.

§ California Institute of Technology.

nearly 100 field ellipticals and *JHK* data alone for galaxies in the Virgo and Coma clusters. These data will allow a more thorough investigation of the color-color and color-magnitude relations discussed here.

II. OBSERVATIONAL PROCEDURES AND DATA REDUCTION

a) *Equipment*

Most of the observations presented in this paper were made during 80 scheduled observing nights at the Hale Observatories in the period 1975 March to 1976 April. The telescopes used were the 24 inch (61 cm), 60 inch (1.5 m), and 100 inch (2.3 m) reflectors on Mount Wilson, and the 200 inch (5 m) Hale reflector. The photometer employed had an offset guider and a star-sky chopper consisting of a rotating sector-wheel mirror near the focal plane. The measurements were made with an InSb detector cooled to 55 K. A similarly cooled iris diaphragm in the focal plane defined the aperture sizes. All of the filters were cooled to 77 K, and have effective wavelengths and full widths at half-maxima as follows: 1.25, 0.24 μm; 1.65, 0.30 μm; 2.20, 0.40 μm; 2.20, 0.11 μm; 2.36, 0.08 μm. The narrow-band 2.20 and 2.36 μm filters define the strength of the 2.3 μm CO absorption band. The fact that these two filters were employed "cold," whereas previously they had been mounted outside the dewar (Frogel *et al.* 1975*b*), caused a shift in the effective wavelength with a consequent decrease in the measured strength of the CO band in a late-type giant relative to that of α Lyrae. This decrease arises almost entirely from the location of the 2.36 μm filter with respect to the CO absorption band, which sets in abruptly at 2.29 μm.[1] It has been found that the relative CO index is insensitive to small changes in the effective wavelength and bandwidth of the 2.20 μm filter (the continuum filter).

Supplemental infrared observations reported in this paper were made on the 0.9 m, 1.3 m, and 2.1 m telescopes of Kitt Peak National Observatory (KPNO), the 40 inch (1 m) telescope of Las Campanas Observatory, Chile, and the 60 inch (1.5 m) telescopes of Cerro Tololo Inter-American Observatory (CTIO) and of the Smithsonian Astrophysical Observatory on Mount Hopkins, Arizona. These observations were made with two additional and completely independent sets of photometer and filters. Transformations which relate the $J - H$ and $H - K$ colors on the different systems are discussed in the Appendix.

b) *Galaxy Observations*

The only galaxies included in the present sample are those early-type systems which were bright enough so that the CO index within a 48″ diameter aperture could be measured on a 1.5 m telescope to a statistical accuracy of better than 0.02 mag in 4–6 hours. With improvements in detector sensitivity, this requirement was met for objects as faint as $K \approx 9.5$. The galaxies include most of the ellipticals and lenticulars for which detailed optical-line indices are available from the work of McClure and van den Bergh (1968), Faber (1973*b*), and O'Connell (1976*a*). Some bright galaxies from these lists and elsewhere were excluded because they lie too close to the galactic plane ($|b| \leq 20°$) or at too southerly a declination ($\delta \lesssim -5°$). Because of uncertainties in the *K*-correction to the CO index, galaxies with redshifts greater than that of the Coma cluster ($z = 0.022$) were not observed. The galaxies observed are listed in Table 1.

All galaxy measurements were made with the focal-plane apertures centered on the optical nuclei. Centering was done visually and usually confirmed by maximizing the 1.65 μm signal. The separation of the "signal" and "reference" beams was typically 2 or 3 aperture diameters. The red Palomar Sky Survey prints were checked for the presence of stars in either of the beams. If any were present, they were measured and an appropriate correction was made in the few cases where the stellar signal was more than a few percent of the galaxian signal. Nearly all of the measurements were repeated on two nights, and the CO indices for the fainter galaxies were measured on as many as five nights on the 60 inch telescope. The night-to-night scatter in the CO index and the broad-band magnitudes was found to be consistent with that expected from the statistical and photometric errors associated with the individual measurements.

c) *Sources of Error and Instrumental Corrections*

In addition to statistical errors from thermal background radiation from the sky and telescope, and from detector noise, a purely photometric error of ± 0.01 mag at all wavelengths was found from repeated measurements of standard stars.

Aside from random errors, several sources of systematic error exist in the raw data. Orthogonal scans of a star across the focal-plane aperture for each of the filters revealed small but measurable differences in the beam profiles for the *J*, *H*, and *K* filters.[2] By convolving a standard galaxy surface-brightness profile (de Vaucouleurs and de Vaucouleurs 1964, hereafter RCBG) with an average of the beam profiles through each of the three filters, we derived corrections to the $J - H$ and $H - K$ colors and to the *K* magnitudes. The corrections to the colors never exceeded 0.06 mag and were typically 0.02 to 0.03 mag. The corrections to the *K* magnitudes were typically 0.00 to 0.01 mag and never exceeded 0.02 mag. The errors associated with these corrections and possible other wavelength-dependent irregularities in the beam profiles are thought to be not larger than ± 0.02 mag. No systematic errors of this type greater than ± 0.01 mag in the CO index could be detected either by scanning the beams or by

[1] Examples of spectra of late-type stars which display the variations of the 2.3 μm CO and 1.9 μm H_2O absorption bands as functions of luminosity and temperature are contained in Moroz (1966), Johnson and Méndez (1970), McCammon, Münch, and Neugebauer (1967), and Frogel (1971).

[2] The usual character of the profiles was that the *K*-filter beam was relatively flat while that of the *J* filter was peaked in the middle. This arises from the wavelength-dependent properties of the silicon field lens.

TABLE 1

Magnitudes and Colors for E and S0 Galaxies

Galaxy / Type (1)	b^{II} / z (2)	Tel. (inches) (3)	Aper. (") (4)	Log A/D(0) (5)	Observed* K (6)	(V-K) (7)	(J-H) (8)	(H-K) (9)	CO (10)	Corrected for Reddening and Redshift K_c (11)	$(V-K)_c$ (12)	$(J-H)_c$ (13)	$(H-K)_c$ (14)	CO_c (15)	Notes (16)
NGC 205	-21°	60	48	-0.98	9.22	2.28:	0.61	0.19	0.09	9.20	2.12:	0.59	0.18	0.095	
S0/E5 pec	-0.0008														
NGC 221	-22	60	16	-1.08	6.92	3.15	0.62	0.21	0.15	6.90	3.00	0.60	0.20	0.15	
E2	-0.0007	60	48	-0.60	5.98	3.31	0.68	0.21	0.16	5.96	3.16	0.66	0.20	0.16	
		24	111	-0.24	5.43	3.28	0.67	0.23	0.14	5.41	3.13	0.65	0.22	0.14	
NGC 404	-27	60	48	-0.38	8.57	2.71:	0.67	0.14	0.11	8.56	2.60:	0.66	0.13	0.11	
$S0_3(0)$	-0.0001														
NGC 584	-68	60	48	-0.33	7.96	3.28	0.68	0.22	0.12	7.98	3.25	0.68	0.20	0.15	
$E3/S0_1(3)$	0.0061	24	111	+0.04	7.68	3.11	0.68	0.18	0.13	7.70	3.08	0.68	0.16	0.16±0.03	
NGC 596	-68	60	48	-0.28	8.62	3.18:	0.64	0.18	0.12	8.64	3.14:	0.64	0.16	0.145	
E0	0.0068														
NGC 1023	-19	60	48	-0.65	7.23	3.30:	0.71	0.21	0.15	7.22	3.10:	0.69	0.19	0.16	
$SB0_1(5)$	0.0019	24	111	-0.28	6.70	3.36	0.68	0.24	0.14	6.69	3.16:	0.66	0.22	0.15	
NGC 1600	-33	200	15	-0.69	9.76	--	0.80	0.31	0.08	9.80	--	0.78	0.26	0.16	
E4	0.0161	60	32	-0.35	9.01	3.49	0.78	0.23	--	9.05	3.33	0.76	0.18	--	
		60	48	-0.18	8.69	3.48	0.69	0.26	0.08	8.73	3.32	0.67	0.21	0.15	
		60	53	-0.14	8.66	3.45	0.74	0.25	--	8.70	3.29	0.72	0.20	--	
NGC 1700	-28	200	15	-0.75	9.27	--	0.74	0.28	0.12	9.31	--	0.72	0.22	0.18	
E3	0.0133	40	28.7	-0.46	8.86	3.30	--	--	--	8.90	3.13	--	--	--	
		60	48	-0.24	8.56	3.32	0.69	0.25	0.11	8.60	3.15	0.67	0.19	0.165	
		40	55.9	-0.17	8.46	3.34	--	--	--	8.50	3.17	--	--	--	
NGC 2300	28	200	15	-0.68	9.19	--	0.78	0.27	0.13	9.21	--	0.77	0.23	0.155	
E3	0.0066	200	16.5	-0.64	9.07	--	0.77	0.26	0.12	9.09	--	0.76	0.22	0.145	
		60	32	-0.35	8.54	3.60:	0.71:	0.24	--	8.56	3.45:	0.70:	0.20	--	
		60	48	-0.18	8.23	3.63:	0.74	0.22	0.13	8.25	3.48:	0.73	0.18	0.155	
		60	53	-0.14	8.18	3.62:	0.74:	0.22	--	8.20	3.47:	0.73:	0.18	--	
		24	111	+0.19	7.87	3.53	0.73	0.19	0.11	7.89	3.38	0.72	0.15	0.14	
NGC 2549	34	200	15	-0.88	9.17	--	0.71	0.25	0.15	9.18	--	0.70	0.23	0.165	
$S0_1(7)$	0.0036	200	16.5	-0.84	9.08	--	0.73	0.23	0.15	9.09	--	0.72	0.21	0.165	
		60	48	-0.38	8.44	3.28	0.59	0.20	0.13	8.45	3.18	0.58	0.18	0.14	
NGC 2634	34	200	15	-0.50	10.22	--	0.72	0.25	0.13	10.24	--	0.71	0.22	0.16	
E1:	0.0066	200	16.5	-0.46	10.10	--	0.70	0.24	0.11	10.12	--	0.69	0.21	0.14±0.03	
		60	48	+0.01	9.50	--	0.69	0.21	0.10	9.52	--	0.68	0.18	0.12	
		60	53	+0.04	9.43	--	0.65	0.27	0.10	9.45	--	0.64	0.24	0.13±0.03	

TABLE 1 - Continued

Galaxy Type (1)	b^{II} z (2)	Tel. (inches) (3)	Aper. (") (4)	Log A/D(0) (5)	Observed* K (6)	(V-K) (7)	(J-H) (8)	(H-K) (9)	CO (10)	Corrected for Reddening and Redshift K_c (11)	$(V-K)_c$ (12)	$(J-H)_c$ (13)	$(H-K)_c$ (14)	CO_c (15)	Notes (16)
NGC 2655	33°	200	15	-1.14	8.80	--	0.70	0.26	0.13	8.81	--	0.69	0.24	0.16	
SAB(s)0	0.0043	60	48	-0.63	7.93	--	0.69	0.24	0.12	7.94	--	0.68	0.22	0.14	
NGC 2672	34	200	15	-0.65	9.82	--	0.76	0.28	0.10	9.86	--	0.74	0.23	0.17	
E2	0.0141	200	16.5	-0.61	9.72	3.46:	0.74	0.30	0.09	9.76	3.30:	0.72	0.25	0.15	
		60	48	-0.15	8.96	3.35:	0.70	0.24	0.10	9.00	3.19:	0.68	0.19	0.16	
NGC 2768	41	200	15	-0.98	9.24	--	0.72	0.25	0.13	9.25	--	0.71	0.23	0.15	
E6	0.0047	200	16.5	-0.94	9.09	--	0.75	0.27	0.15	9.10	--	0.74	0.25	0.165	
		60	48	-0.48	8.14	3.31	0.71	0.19	0.15	8.15	3.23	0.70	0.17	0.165	
		24	111	-0.11	7.48	3.34:	0.69	0.19	0.12	7.49	3.26:	0.68	0.17	0.14±0.04	
NGC 2974	35	200	15	-0.75	9.08	--	0.76	0.26	0.13	9.09	--	0.75	0.23	0.155	
E4	0.0067														
NGC 3115	37	200	15	-1.04	7.58	3.56	0.73	0.25	0.15	7.58	3.49	0.72	0.24	0.16	
E7/SO_1(7)	0.0022	50	31.6	-0.72	7.02	3.42	0.71	0.24	--	7.02	3.35	0.70	0.23	--	
		84	37.5	-0.64	6.89	3.39	0.68	0.24	0.17	6.89	3.32	0.67	0.23	0.17	
		60	48	-0.54	6.73	3.39	0.71	0.22	0.18	6.73	3.32	0.70	0.21	0.185	
		36	106.4	-0.19	6.27	3.35	0.72	0.23	0.17	6.27	3.28	0.71	0.22	0.175	
NGC 3158	55	200	15	-0.56	9.99	--	0.76	0.30	--	10.07	--	0.75	0.22	--	
E3	0.0234	200	16.5	-0.52	9.89	--	0.73	0.32	0.05	9.97	--	0.72	0.24	0.16	
NGC 3193	55	200	15	-0.78	9.26	--	0.70	0.23	0.14	9.28	--	0.70	0.21	0.16	
E2	0.0046	200	16.5	-0.74	9.13	--	0.73	0.24	0.15	9.15	--	0.73	0.22	0.165	
		60	48	-0.28	8.49	3.19	0.67	0.20	0.15	8.51	3.16	0.67	0.18	0.17	
NGC 3226	55	200	15	-0.77	9.91	--	0.73	0.24	--	9.93	--	0.73	0.22	--	
E2	0.0045	200	16.5	-0.73	9.79	--	0.75	0.26	0.13	9.81	--	0.75	0.24	0.14	
		60	48	-0.27	9.11	--	0.68	0.23	0.12	9.13	--	0.68	0.21	0.135	
		24	111	+0.10	8.57	--	0.63	0.20	0.11	8.59	--	0.63	0.18	0.12±0.05	
NGC 3377	58	200	15	-0.90	8.92	3.18	0.70	0.22	0.16	8.93	3.17	0.70	0.21	0.17	
E6	0.0024	40	28.7	-0.62	8.52	3.07	--	--	--	8.53	3.06	--	--	--	
		40	55.9	-0.33	8.10	3.03	--	--	--	8.11	3.02	--	--	--	
NGC 3379	58	200	15	-0.96	8.10	3.34	0.72	0.25	0.14	8.11	3.33	0.72	0.24	0.15	
E0	0.0029	50	31.6	-0.64	7.51	3.34	0.70	0.22	--	7.52	3.33	0.70	0.21	--	
		60	48	-0.46	7.19	3.39	0.68	0.21	0.15	7.20	3.38	0.68	0.20	0.155	
		24	111	-0.09	6.69	3.35	0.68	0.19	0.16	6.70	3.34	0.68	0.18	0.17	
NGC 3384	58	200	15	-1.01	8.25	3.28	0.70	0.24	0.15	8.26	3.27	0.70	0.22	0.16	
$SB0_1$(5)	0.0026	40	28.7	-0.73	7.85	3.22	--	--	--	7.86	3.21	--	--	--	
		50	31.6	-0.69	7.80	3.22	0.68	0.24	--	7.81	3.21	0.68	0.22	--	
		40	55.9	-0.44	7.50	3.18	--	--	--	7.51	3.17	--	--	--	

TABLE 1 - Continued

Galaxy Type (1)	b^{II} z (2)	Tel. (inches) (3)	Aper. (") (4)	Log A/D(0) (5)	Observed* K (6)	(V-K) (7)	(J-H) (8)	(H-K) (9)	CO (10)	Corrected for Reddening and Redshift K_c (11)	$(V-K)_c$ (12)	$(J-H)_c$ (13)	$(H-K)_c$ (14)	CO_c (15)	Notes (16)
NGC 3607	66°	200	15	-0.83	8.58	3.55:	0.73	0.27	0.15	8.60	3.53:	0.73	0.25	0.16	
SO_3 (3)	0.0031	50	31.6	-0.50	8.02	3.40:	0.70	0.25	--	8.04	3.38:	0.70	0.23	--	
		60	48	-0.32	7.73	3.37:	0.69	0.22	0.15	7.75	3.35:	0.69	0.20	0.16	
		60	53	-0.27	7.62	3.40:	0.67	0.25	0.16	7.64	3.38:	0.67	0.23	0.175	
NGC 3608	67	200	15	-0.70	9.36	3.40:	0.70	0.24	0.13	9.38	3.38:	0.70	0.22	0.14	
E1	0.0040	60	48	-0.20	8.55	3.23	0.70	0.22	0.15	8.57	3.21	0.70	0.20	0.17	
		60	53	-0.16	8.47	3.25	0.69	0.22	0.11	8.49	3.23	0.69	0.20	0.125	
NGC 3613	55	200	16.5	-0.76	9.20	--	0.72	0.25	0.13	9.23	--	0.72	0.22	0.155	
E6	0.0069	60	48	-0.30	8.52	3.20:	0.66	0.20	0.13	8.55	3.15:	0.66	0.17	0.155	
NGC 3842	73	200	16.5	--	10.25	--	0.76	0.30	0.03	10.32	--	0.75	0.23	0.13	1
E	0.0206	60	48	--	9.43	--	0.58	0.26	0.04	9.50	--	0.57	0.19	0.13	
NGC 3998	60	200	15	-0.83	8.46	3.52:	0.73	0.27	0.14	8.47	3.50:	0.73	0.25	0.15	
SO_1 (3)	0.0036														
NGC 4261	67	200	16.5	-0.87	8.83	3.45	0.75	0.28	0.15	8.86	3.41	0.75	0.25	0.175	
E3	0.0073	60	48	-0.41	8.05	3.35	0.70	0.22	0.14	8.08	3.31	0.70	0.19	0.17	
NGC 4278	83	200	7.5	-1.17	9.37	--	0.70	0.25	0.14	9.38	--	0.70	0.24	0.15	
E1	0.0021	200	15	-0.87	8.65	--	0.74	0.25	0.14	8.66	--	0.74	0.24	0.145	
		200	16.5	-0.82	8.50	--	0.75	0.24	0.16	8.51	--	0.75	0.23	0.17	
		50	31.6	-0.54	8.10	3.28	0.72	0.17	--	8.11	3.27	0.72	0.16	--	
		60	48	-0.36	7.81	3.29	0.61	0.22	0.14	7.82	3.28	0.61	0.21	0.15	
		60	53	-0.32	7.69	3.35	0.67	0.21	0.19	7.70	3.34	0.67	0.20	0.20	
		24	111	+0.01	7.38	3.23	0.64	0.21	0.15	7.39	3.22	0.64	0.20	0.16	
NGC 4283	83	200	16.5	-0.49	9.73	--	0.71	0.25	0.21	9.75	--	0.71	0.23	0.22	
E0	0.0036	60	48	-0.03	9.26	3.24	0.62	0.25	0.13	9.28	3.22	0.62	0.23	0.14	
NGC 4365	69	200	15	-1.09	8.73	3.37	0.73	0.26	0.15	8.74	3.35	0.73	0.24	0.16	
E3	0.0039	40	28.7	-0.81	8.20	3.29	--	--	--	8.21	3.27	--	--	--	
		50	31.6	-0.77	8.18	3.25	0.68	0.26	--	8.19	3.23	0.68	0.24	--	
		40	55.9	-0.52	7.59	3.31	--	--	--	7.60	3.29	--	--	--	
NGC 4374	74	200	7.5	-1.28	9.17	--	0.70	0.21	0.15	9.18	--	0.70	0.20	0.16	
E1 pec	0.0032	200	15	-0.98	8.27	3.47	0.72	0.25	0.10	8.28	3.46	0.72	0.24	0.11	
		50	31.6	-0.66	7.59	3.36	0.69	0.25	--	7.60	3.35	0.69	0.23	--	
		60	48	-0.48	7.29	3.31	0.71	0.21	0.16	7.30	3.30	0.71	0.20	0.165	
		60	53	-0.44	7.15	3.38	0.69	0.24	0.16	7.16	3.37	0.69	0.23	0.17	

TABLE 1 - Continued

Galaxy / Type (1)	b^{II} / z (2)	Tel. (inches) (3)	Aper. (") (4)	Log A/D(0) (5)	Observed* K (6)	(V-K) (7)	(J-H) (8)	(H-K) (9)	CO (10)	Corrected for Reddening and Redshift K_c (11)	$(V-K)_c$ (12)	$(J-H)_c$ (13)	$(H-K)_c$ (14)	CO_c (15)	Notes (16)
NGC 4382	79°	200	15	-1.20	8.62	3.09	0.73	0.23	0.13	8.63	3.08	0.73	0.21	0.135	
SO_1(3)	0.0026	40	28.7	-0.92	8.06	3.03	--	--	--	8.07	3.02	--	--	--	
		50	31.6	-0.88	7.95	3.09	0.67	0.25	--	7.96	3.08	0.67	0.23	--	
		40	55.9	-0.63	7.44	3.04	--	--	--	7.45	3.03	--	--	--	
NGC 4406	75	200	7.5	-1.37	9.48	--	0.70	0.20	0.15	9.49	--	0.70	0.19	0.15	
E2	-0.0010	200	15	-1.07	8.75	3.29	0.71	0.26	0.16	8.76	3.28	0.71	0.25	0.16	
		50	31.6	-0.75	8.04	3.21	0.67	0.21	--	8.05	3.20	0.67	0.20	--	
		60	48	-0.57	7.57	3.26	0.68	0.22	0.18	7.58	3.25	0.68	0.21	0.18	
NGC 4459	76	200	15	-0.81	8.76	3.69	0.76	0.29	0.13	8.77	3.67	0.76	0.27	0.14	
SO_3(3)	0.0037	40	28.7	-0.53	8.35	3.39	--	--	--	8.36	3.37	--	--	--	
		40	55.9	-0.24	7.84	3.35	--	--	--	7.85	3.32	--	--	--	
NGC 4464	70	200	16.5	-0.51	10.05	--	0.70	0.20	0.11	10.07	--	0.70	0.18	0.125	
E3	0.0040	60	48	-0.05	9.69	3.11:	0.71	0.15	0.17	9.71	3.09:	0.71	0.13	0.18±0.04	
NGC 4472	70	200	7.5	-1.56	9.16	--	0.70	0.23	0.16	9.17	--	0.70	0.22	0.165	
E2	0.0032	200	15	-1.26	8.19	3.42	0.75	0.27	0.16	8.20	3.41	0.75	0.26	0.175	
		200	16.5	-1.21	8.00	3.44	0.75	0.28	0.15	8.01	3.43	0.75	0.27	0.165	
		50	31.6	-0.93	7.37	3.30	0.70	0.24	--	7.38	3.29	0.70	0.23	--	
		60	48	-0.75	6.91	3.32	0.65:	0.22	0.16	6.92	3.31	0.65:	0.21	0.165	
		24	111	-0.38	6.18	3.39	0.68	0.24	0.15	6.19	3.38	0.68	0.23	0.16	
NGC 4478	74	200	15	-0.65	9.54	--	0.69	0.24	0.12	9.55	--	0.69	0.22	0.14	
E2	0.0049	H60	27.4	-0.39	8.92	3.32:	0.63	0.22	--	8.93	3.29:	0.63	0.20	--	
		H60	53.4	-0.10	8.51	3.29	0.64	0.20	--	8.52	3.26	0.64	0.18	--	
NGC 4486	74	200	7.5	-1.48	9.76	--	0.73	0.23	0.15	9.78	--	0.73	0.21	0.165	
E0	0.0042	200	15	-1.18	8.59	3.26	0.76	0.29	0.14	8.61	3.24	0.76	0.27	0.16	
		50	31.6	-0.86	7.60	3.38	0.73	0.24	--	7.62	3.36	0.73	0.22	--	
		60	48	-0.68	7.08	3.42	0.73	0.25	0.16	7.10	3.40	0.73	0.23	0.175	
		24	111	-0.31	6.37	3.41	0.65	0.25	0.15	6.39	3.39	0.65	0.23	0.16	
NGC 4486A	74	200	7.5	--	10.02	--	0.51	0.10	0.09	10.03	--	0.51	0.08	0.11	
	(0.004)	200	15	--	9.52	--	0.52	0.17	0.10	9.53	--	0.52	0.15	0.115	2
NGC 4486B	75	200	7.5	-0.40	10.61	--	0.74	0.16	0.11	10.62	--	0.74	0.14	0.13	
E0	0.0050	200	15	-0.10	10.23	--	0.68	0.21	0.08	10.24	--	0.68	0.19	0.10	
NGC 4494	85	60	48	-0.38	7.96	3.09:	0.68	0.20	0.12	7.98	3.06:	0.68	0.18	0.135	
E1	0.0044	24	111	-0.01	--	--	--	--	0.10	--	--	--	--	0.115	
NGC 4649	74	200	15	-1.10	8.14	3.50	0.73	0.28	0.16	8.16	3.47	0.73	0.26	0.17	
E2/S0	0.0042	50	31.6	-0.76	7.34	3.42	0.74	0.24	--	7.36	3.39	0.74	0.22	--	
		60	48	-0.60	6.93	3.42	0.65:	0.23	0.16	6.95	3.39	0.65:	0.21	0.175	

TABLE 1 - Continued

Galaxy / Type (1)	b^{II} / z (2)	Tel. (inches) (3)	Aper. (") (4)	Log A/D(0) (5)	Observed* K (6)	(V-K) (7)	(J-H) (8)	(H-K) (9)	CO (10)	Corrected for Reddening and Redshift K_c (11)	$(V-K)_c$ (12)	$(J-H)_c$ (13)	$(H-K)_c$ (14)	CO_c (15)	Notes (16)
NGC 4889	88°	200	15	-0.71	9.99	3.41	0.75	0.28	0.08	10.06	3.30	0.74	0.21	0.175	
E4	0.0215	200	16.5	-0.66	9.85	3.45	0.72:	0.33	0.07	9.92	3.34	0.71:	0.26	0.17	
		60	48	-0.20	9.06	3.41	0.70	0.29	0.06	9.13	3.30	0.69	0.22	0.16	
NGC 5813	50	200	15	-0.86	9.36	--	0.71	0.26	0.11	9.39	--	0.71	0.23	0.13	
E1	0.0063	200	16.5	-0.82	9.22	--	0.72:	0.25	0.11	9.25	--	0.72:	0.22	0.14	
		50	31.6	-0.54	8.74	3.46	0.66	0.25	--	8.77	3.39	0.66	0.22	--	
		60	32	-0.53	8.72	3.46	0.67	0.25	--	8.75	3.39	0.67	0.22	--	
		60	48	-0.36	8.43	3.47	0.71	0.24	0.13	8.46	3.40	0.71	0.21	0.15	
		60	53	-0.32	8.32	3.51	0.70	0.26	--	8.35	3.44	0.70	0.23	--	
NGC 5846	49	200	16.5	-0.86	9.13	3.54	0.74	0.28	0.15	9.16	3.47	0.74	0.25	0.17	
E1	0.0059	50	31.6	-0.58	8.46	3.50	0.67	0.25	--	8.49	3.43	0.67	0.22	--	
		60	32	-0.57	8.38	3.56	0.67	0.26	--	8.41	3.49	0.67	0.23	--	
		60	48	-0.40	8.03	3.53	0.75	0.24	0.13	8.06	3.46	0.75	0.21	0.15	
		60	53	-0.36	7.89	3.58	0.72	0.27	--	7.92	3.51	0.72	0.24	--	
		24	111	-0.03	7.23	3.59	0.75	0.28	0.14	7.26	3.52	0.75	0.25	0.17±0.03	
NGC 5866	52	100	30	-0.66	7.96	3.42:	0.66	0.32	0.12	7.98	3.40:	0.66	0.30	0.135	
SO_3 (8)	0.0026	50	31.6	-0.64	7.93	3.38:	0.74	0.29	--	7.95	3.36:	0.74	0.27	--	
		60	48	-0.46	7.59	3.49:	0.68	0.30	0.16	7.61	3.47:	0.68	0.28	0.17	
		60	53	-0.41	7.49	3.50:	0.72	0.30	--	7.51	3.48:	0.72	0.28	--	
NGC 5982	47	200	7.5	-0.95	10.02	--	0.71	0.23	0.13	10.06	--	0.70	0.19	0.17	
E3	0.0096	200	15	-0.65	9.30	3.40	0.71	0.27	0.13	9.34	3.31	0.70	0.23	0.17	
		100	30	-0.35	8.85	3.30	0.67	0.24	0.13	8.89	3.21	0.66	0.20	0.17	
		60	48	-0.15	8.59	3.25	0.59:	0.22	0.14	8.63	3.16	0.58:	0.18	0.185	
		60	53	-0.11	8.48	3.32	0.66	0.26	0.14	8.52	3.23	0.65	0.22	0.18±0.04	
		24	111	+0.22	8.22	3.27	0.66	0.20	0.10	8.26	3.18	0.65	0.16	0.14±0.06	
NGC 6702	20	60	32	-0.15	9.75	3.60:	--	--	--	9.78	3.35:	--	--	--	
E2	0.0158	60	48	+0.02	9.53	3.61:	0.73	0.29	0.13	9.56	3.36:	0.70	0.23	0.21	
		60	53	+0.06	9.51	3.57:	0.72	0.30	--	9.54	3.32:	0.69	0.24	--	
NGC 7619	-48	60	16	-0.63	9.27	--	0.69	0.25	0.11	9.32	--	0.68	0.20	0.17	
E3	0.0125	60	48	-0.16	8.53	3.59:	0.71	0.26	0.11	8.58	3.49:	0.70	0.21	0.17	
		24	111	+0.21	8.09	3.42:	0.75	0.24	0.10	8.14	3.32:	0.74	0.19	0.16±0.05	
NGC 7626	-48	60	48	-0.12	8.70	3.50	0.71	0.23	0.11	8.74	3.41	0.70	0.19	0.17	
E1	0.0112														

*The assigned nominal errors are ±0.03, ±0.10, ±0.04, ±0.03, and ±0.02 for K, (V-K), (J-H), (H-K), and CO, respectively. A colon indicates that the error for that measurement may be as much as twice the nominal value. CO index errors larger than ±0.02 are indicated in the body of the table.

NOTES: 1. This galaxy is from the list of Gunn and Oke (1975). 2. The redshift was assumed to be the same as for N 4486.

measuring a standard star at several positions in the aperture.[3]

Possible errors from other *known instrumental* sources are believed to be of the order of 0.01 mag in the mean. These include the correction to the K magnitude for galaxian flux in the reference beam (Frogel *et al.* 1975*c*) and nonlinearity in the response of the system to bright and faint standards. An intercomparison of the same standards measured on the 0.6 m, 1.5 m, and 5 m telescopes was used as a monitor of possible nonlinear response effects. A linearity problem in our previously published CO indices (Frogel *et al.* 1975*b*) is discussed in § II*f*.

The observed K magnitudes and colors corrected for the instrumental effects discussed above are given in columns (6), (8), and (9) of Table 1. The CO indices in column (10) have had no instrumental corrections applied. The adopted errors are listed at the bottom of Table 1. These errors are consistent with the scatter in repeated measurements *after* the application of the instrumental corrections.

d) *Sources of V Data*

The visual magnitudes used in column (7) of Table 1 are based largely upon a compilation from the literature by Sandage (1976). We have also included data from Tifft (1969, 1973). As described in Frogel *et al.* (1975*c*), values for V at apertures corresponding to those at which the infrared measurements were made were interpolated from the tabulated data. Errors in $V-K$, from uncertainties in combining measurements made with different aperture sizes, and from scatter in the published V data, are estimated to be ± 0.10 mag. A colon after a $V-K$ color in Table 1 indicates that the scatter in the published V data is exceptionally large; for these cases we adopt an error in $V-K$ of ± 0.2 mag. In addition, a systematic error could be present in the 200 inch $V-K$ colors which depend on a relatively limited amount of published small-aperture V data. A few galaxies had no appropriate V measurements available from the literature. Data for some of these were taken from *UBVR* measurements made on the 0.9 m and 1.5 m telescopes at CTIO (Paper III). Clearly, the use of such a heterogeneous body of V data will hinder our examination of variations in the $V-K$ color *within* galaxies, since these variations are small to begin with (see Frogel *et al.* 1975*c*).

e) *Reddening and K-Corrections*

To obtain the reddening and extinction corrections, the absorption-free polar-cap model for A_V given by Sandage (1973) was used together with the van de Hulst reddening law (Johnson 1966*c*). The values of E_{J-H}/A_V, E_{H-K}/A_V, E_{V-K}/A_V, E_{U-V}/A_V, and E_{CO}/A_V used are 0.10, 0.06, 0.91, 0.56, and 0.00, respectively. Since the largest value of A_V was only 0.21 mag, errors which may arise from the inapplicability of either the polar-cap model or the van de Hulst reddening law cannot affect the conclusions of this paper.

The K-corrections to the V magnitudes are from Schild and Oke (1971) and Whitford (1971). (For the limited redshift range of the galaxies considered here, the results of both authors are identical.) For the $U-V$ colors obtained from the literature, the K-correction is from Table 3 of Sandage (1972). Heliocentric redshifts (column [2], Table 1) are from RCBG.

Separate procedures were followed for determining the K-correction for the infrared broad-band data and for the CO index. The stratoscope balloon scans of several late-type stars (Woolf, Schwarzschild, and Rose 1964) were convolved with the transmission curves of the *JHK* filters and redshifted. The resulting K-corrections as functions of z were quite similar for α Tau (K5 III), μ Gem (M3 III), and α Ori (M2 I)—the spread at $z = 0.03$ was only 0.01 to 0.02 mag in the $J-H$ and $H-K$ colors and K magnitudes. Since the CO indices of nearby galaxies are most similar to those of a late K III star, the values for α Tau were used to correct the broad-band galaxy measurements. The K-corrections are approximately linear with increasing z; for $z = 0.03$ they are -0.02, -0.10, and $+0.10$ for $J-H$, $H-K$, and K, respectively.

Redshift corrections to the CO index were first determined numerically by convolving the transmission curves of the two filters with the high-resolution spectra of several stars observed by Frogel (1971). For K2, K5, and M2 giants, the corrections were similar out to a z of 0.012. Beyond this they diverged rapidly; the spread becomes nearly 0.04 mag at $z = 0.022$. Uncertainty in the choice of a realistic starting point (i.e., a model stellar population) therefore made it necessary to derive empirically the K-correction to the CO index at large redshift. We show below that the CO index depends only weakly on galaxian luminosity or radius for the brighter nearby galaxies. Thus the *observed* CO indices of the intrinsically brightest galaxies were plotted against redshift, and a straight-line fit to the data was made. The K-correction found in this way, and adopted for all galaxies, is given by $K_{CO} = +4.8z$. Out to $z = 0.012$ the empirical relation agreed with the mean computed relation for the three stars to better than ± 0.01 mag. Although the empirical relation is based on observations of the most luminous galaxies, no systematic error is introduced in the results for fainter galaxies, since they are all at small values of z. (See Lasker 1970 for a discussion of this point.) *Note that for galaxies in the Coma cluster the K-correction is two-thirds of the final CO index.*

f) *Comparisons with Previous* CO *Measurements*

The CO observations presented in this paper were made on the photometric system described above and defined by the standards listed in Table 10. By re-observing with the new ("cold") system many of the stars used to define Figure 1 of Frogel *et al.* (1975*b*) (the old, "warm" system), and by making simul-

[3] The measurements made on the 1.3 m telescope at KPNO employed an off-axis field mirror rather than a field lens. Thus the beam profiles were the same at all wavelengths, and no corrections to the *colors* were required. Corrections to the K magnitudes were found to be of the order of -0.03 mag.

taneous observations on both old and new systems for 16 giant stars, we determined the transformation of the CO index from the warm to the cold system to be

$$\text{CO index: Warm} - \text{Cold} = 0.1 \times \text{Warm} \qquad \text{Warm} \leq 0.2$$

$$\text{Warm} - \text{Cold} = 0.02 \qquad \text{Warm} > 0.2$$

i.e., the sense of the transformation is that the CO indices for the giants and supergiants in Figure 1 of Frogel *et al.* (1975*b*) become *smaller*. The error in the transformation as determined from the scatter of stellar measurements is of the order of the size of the transformation. *This transformation applies only to giants and supergiants.*

All of the galaxies measured on the old system were remeasured with the new system. For the data obtained with the 5 m telescope, a comparison with the measurements reported in Table 1 of Frogel *et al.* (1975*b*) revealed that *even after the old* CO *indices were transformed*, the resulting values for the CO index were larger than the new values by 0.04 mag in the mean. Reexamination of the old data indicated that the source of most of this systematic difference was due to saturation of the continuum signal from bright standards. The continuum filter (2.20 μm) gave a signal nearly 3 times as strong as the CO filter, and the signal through the former was clipped by about 0.03 mag. The effect of this was to assign too strong a CO index to the galaxies. Old measurements made with the 1.5 m telescope (Frogel *et al.* 1975*b* and unpublished data) were also transformed to the "cold" system and compared with measurements reported here. No statistically significant differences were found. We emphasize that the systematic differences in the 200 inch measurements *in no way affect the main conclusion of the earlier paper*. The one consequence of the error in these measurements was to give a false impression of the existence of a radial gradient in the CO index (Frogel *et al.* 1975*a*, *b*). The galaxy data presented here supersede these previously published CO data.

The K magnitudes of all galaxies in Frogel *et al.* (1975*c*) were remeasured in the course of this work. There is no systematic difference larger than 0.01 mag in the mean between these two independent sets of data.

g) Globular-Cluster Observations

The integrated infrared light of five globular clusters was observed with the KPNO 0.9 m and the CTIO 1.5 m telescopes. Reference beam corrections were derived by using the multiaperture photometry of Kron and Mayall (1960) with the assumption of no radial color dependence. For M13, the correction to the K magnitude was -0.11 mag; for the other clusters, it was between -0.03 and -0.05 mag. Corrections to the infrared measurements for nonuniformity in the beam profiles were calculated in a manner similar to that employed for the galaxy measurements, and amounted to a few hundredths of a magnitude. $V - K$ colors were formed by using V magnitudes interpolated from the data of Kron and Mayall (1960) and transformed to the Johnson V system (Peterson and King 1975). Values of E_{B-V} are from van den Bergh (1967) for M69 and M15, and are those recommended by Sandage (1970) for the others. $U - V$ values are also from van den Bergh (1967), although not at the same aperture sizes as the infrared measurements. Final values with all corrections applied are presented in Table 2.

III. DISCUSSION OF THE GALAXY OBSERVATIONS

Table 1 contains the final colors and magnitudes of the galaxies corrected for reddening and redshift. Many of the morphological types are from Sandage (1976). Values of log $A/D(0)$ refer to the aperture size in units of the major diameter $D(0)$ (RCBG). We first consider the variations of the different photometric indices within individual galaxies. This then permits discussion of the average galaxian colors within a standard projected aperture size. The reader should bear in mind the restricted nature of the sample of galaxies, particularly with regard to their absolute magnitude. Also, multiaperture observations such as those presented here are not ideal for a study of color gradients within galaxies. Since such gradients are expected to be small in most cases, and since the accuracy of the photometric measurements is never better than a few percent, the galaxies can be treated

TABLE 2

GLOBULAR-CLUSTER DATA

Cluster	Aperture	[Fe/H]†	Observed*			Reddening Corrected					
			K	$J-H$	$H-K$	K	$U-V$	$V-K$	$J-H$	$H-K$	CO
M3	105.	−1.5	5.23	0.49	0.08	5.23	0.78	2.16	0.49	0.08	+0.01
M13	105.	−1.6	5.05	0.54	0.09	5.04	0.66	2.41	0.53	0.08	+0.03
M15	105.	−1.9	4.97	0.49	0.09	4.94	0.55	1.82	0.46	0.07	+0.01
M69	66.4	> −0.4	5.62	0.70	0.17	5.57	1.15	2.59	0.64	0.13	+0.08
M92	105.	−2.2	5.25	0.47	0.08	5.25	0.61	2.15	0.47	0.07	−0.01

* The "observed" values have been corrected for beam profile and reference beam flux, as discussed in the text. The CO values did not require any corrections.

† For M3, M13, M15, and M92, [Fe/H] is from Hesser, Hartwick, and McClure 1976. For M69, [Fe/H] is an estimate based on the results of Hartwick and Sandage 1968.

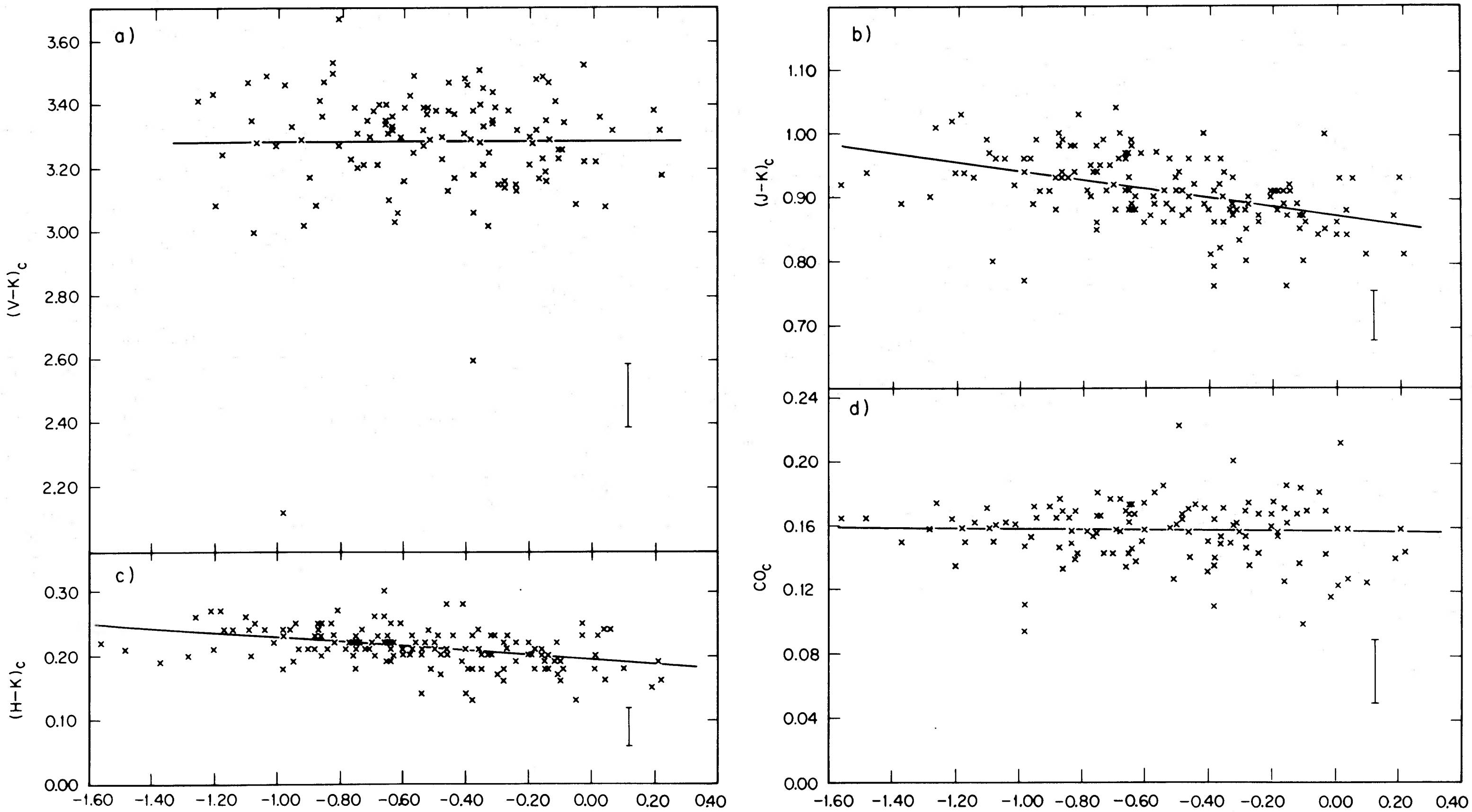

FIG. 1.—All the corrected colors and CO indices from Table 1 are plotted as a function of log $A/D(0)$. The linear least-squares fit to these data points is shown by the solid line and is discussed in the text.

TABLE 3

RADIAL COLOR GRADIENTS

	All-Points Solution (Fig. 1)				Average of Individual Radial Gradients			
Color	N	Slope	$\pm\sigma_m$	r	N	Slope	$\pm\sigma_m$	$\pm\sigma_e$
CO............	120	−0.002	(0.01)	−0.05	33	0.00	(0.01)	0.02
$V-K$.........	120	0.00	(0.03)	0.00	32	−0.11	(0.04)	0.05
$J-H$.........	148	−0.04	(0.01)	−0.34	37	−0.08	(0.01)	0.04
$H-K$.........	148	−0.04	(0.01)	−0.43	37	−0.04	(0.01)	0.03
$J-K$.........	148	−0.07	(0.01)	−0.46	37	−0.12	(0.02)	0.04

NOTES.—The all-points solution on the left gives the slope Δ color/Δ log $A/D(0)$ for galaxies in Table 1 and Fig. 1; r is the correlation coefficient. The averages of individually determined color gradients are given on the right. In the last two columns are listed the purely statistical errors (σ_m), and our estimated errors (σ_e) in the slope values. The estimated errors include contributions from possible systematic beam profile effects as discussed in the text.

only in a statistical sense and not examined individually. A much better technique is to displace the measuring aperture from the center of the galaxy (e.g., Strom *et al.* 1976, 1977).

a) *The Dependence of Color and* CO *Index on Radius*

Figure 1 displays all the galaxy observations from Table 1 as a function of log $A/D(0)$.

Table 3 presents least-squares solutions for radial color gradients found in two ways. First, linear fits [color versus log $A/D(0)$] were made to all of the data in Table 1 treated simultaneously; these fits are plotted in Figure 1. Second, slopes and errors were found for each galaxy individually, and then a weighted average was taken. Owing to the magnitude-limited nature of the sample, selection effects could influence the first solution; only the solutions on the right side of Table 3 have physical significance. As mentioned above, the 5 m $V-K$ colors may contain a small systematic error. Although exclusion of these data does not produce a statistically significant change in the mean $V-K$ gradient, the uncertainty in the gradient for this solution becomes as large as the gradient itself.

Two important results from Table 3 are that (1) the broad-band colors become bluer with increasing aperture size, and (2) there is no radial gradient in the CO index. The latter result differs from the tentative conclusion of Frogel *et al.* (1975*b*), as discussed in § II*f*. The former result for the $V-K$ color is consistent, to within the errors, with that of Frogel *et al.* (1975*c*). Note, however, that, to within the errors, the mean radial change in $V-K$ can be entirely accounted for by the change in $J-K$. The variances of the fits are consistent with the measuring errors for $J-H$, $H-K$, and CO, while for $V-K$ it is about twice the estimated errors.

The dependence of $V-K$ on aperture size is not well established by the data of this paper. At least part of the problem lies in the heterogeneous nature of the V data, as mentioned. Also, we cannot rule out a large dispersion in the $V-K$ gradients of individual galaxies. The average $J-K$ gradient (Table 3) is large, however, and seems to indicate that any such dispersion would have to occur shortward of 1 μm.

Another estimate of the *average* dependence of $V-K$ color on aperture size can be made by comparing V and K growth curves. Figure 2 displays the K growth curve obtained from the present data (see § III*b*). This curve was compared with a V growth curve constructed from data to be presented in Paper III. This latter curve is based on a *homogeneous* set of multiaperture observations made at CTIO of about 100 E and S0 galaxies. In terms of the distribution in absolute magnitude, this sample is similar to the sample studied here. It differs, however, in consisting primarily

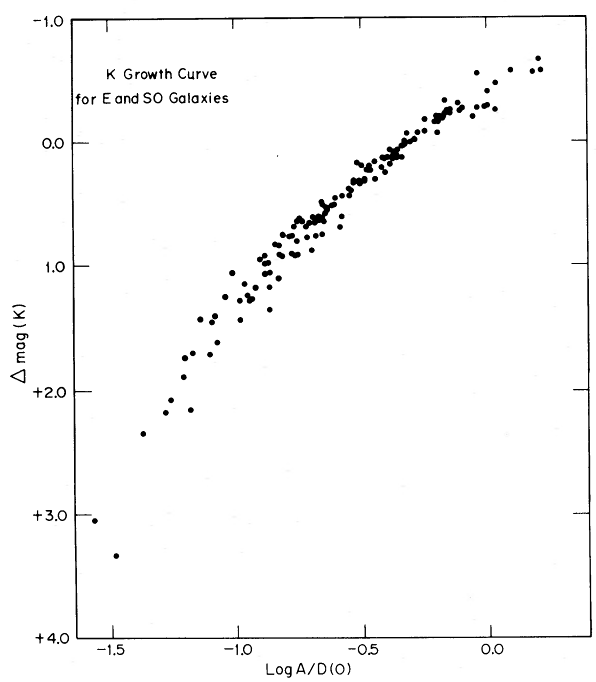

FIG. 2.—The K growth curve based on the data of Table 1 and derived as discussed in the text. Normal points for the mean curve are given in Table 5.

TABLE 4

Fully Corrected Colors and Magnitudes for E and S0 Galaxies

Galaxy	CO	Values at A/D(0) = 0.5					Values at A/D(0) = 1.0			Notes
		$(U-V)_{0.5}$	$(V-K)_{0.5}$	$(J-K)_{0.5}$	$(H-K)_{0.5}$	$K_{0.5}$	$V_{1.0}$	$M_{V1.0}$	$M_{K1.0}$	
(1)	(2)	(3)	(4)	(5)	(6)	(7)	(8)	(9)	(10)	(11)
NGC 205	0.095	0.81	2.12	0.71	0.15	7.9	8.72	-15.38	-16.6	2,5,6
221	0.155	1.31	3.14	0.87	0.21	5.50	8.16	-15.94	-19.02	1,5
404	0.11	1.03	2.60	0.78	0.13	8.44	10.44	-13.66	-16.08	2,5,6
584	0.15	1.52	3.24	0.88	0.20	7.95	10.81	-22.11	-25.39	1
596	0.145	1.43	3.14	0.80	0.16	8.65	11.42	-21.50	-24.69	1,2,6
1023	0.16	1.46	3.15	0.88	0.22	6.72	9.44	-21.06	-24.20	
1600	0.155	1.53	3.33	0.93	0.20	8.93	11.75	-23.16	-26.40	1
1700	0.17	1.38	3.15	0.87	0.19	8.68	11.41	-23.03	-26.18	1
2300	0.15	1.64	3.46	0.92	0.19	8.45	11.52	-21.88	-25.37	1
2549	0.155	1.49	3.18	0.75	0.17	8.26	11.28	-20.39	-23.83	
2634	0.14	--	--	0.89	0.20	9.92	--	--	--	
2655	0.15	--	--	0.87	0.21	7.38	10.27	-21.79	-25.10	
2672	0.16	1.53	3.22	0.90	0.21	9.25	12.10	-22.42	-25.69	
2768	0.16	1.50	3.24	0.87	0.17	7.82	10.57	-22.06	-25.23	1
2974	0.155	1.54	3.43	0.94	0.21	8.3	11.26	-21.52	-24.9	2,4,6
3115	0.17	1.59	3.30	0.93	0.22	6.33	9.33	-20.29	-23.71	1
3158	0.16	1.62	3.44	0.94	0.22	9.5	12.59	-23.15	-26.7	1,2,4,6
3193	0.165	1.46	3.16	0.85	0.18	8.53	11.24	-20.66	-23.79	1
3226	0.14	1.48	3.32	0.89	0.21	9.17	11.85	-20.05	-23.15	4
3377	0.17	1.22	3.02	0.85	0.19	7.99	10.68	-20.20	-23.31	6
3379	0.155	1.63	3.36	0.87	0.19	6.97	9.87	-21.01	-24.33	
3384	0.16	1.45	3.15	0.87	0.22	7.20	10.20	-20.68	-24.10	1,6
3607	0.165	1.52	3.36	0.90	0.21	7.70	10.64	-20.97	-24.33	1
3608	0.145	1.48	3.24	0.90	0.20	8.73	11.45	-20.16	-23.30	1
3613	0.155	1.47	3.15	0.83	0.17	8.55	11.19	-21.68	-24.74	
3842	0.13	--	--	--	--	--	--	--	--	3
3998	0.15	1.50	3.50	0.93	0.23	7.5	10.83	-21.02	-24.8	1,2,6
4261	0.175	1.60	3.29	0.88	0.22	7.88	10.86	-22.32	-25.72	
4278	0.165	1.45	3.29	0.86	0.20	7.68	10.62	-20.73	-24.09	1
4283	0.18	1.37	3.22	0.90	0.23	9.56	12.50	-18.85	-22.21	
4365	0.16	1.57	3.29	0.90	0.24	7.29	10.03	-21.70	-24.86	1
4374	0.15	1.56	3.33	0.89	0.21	7.00	9.87	-21.86	-25.15	1
4382	0.135	1.41	3.05	0.85	0.21	6.89	9.40	-22.33	-25.26	1
4406	0.17	1.52	3.23	0.88	0.21	7.15	9.79	-21.94	-25.00	1
4459	0.14	1.53	3.33	0.98	0.25	8.02	10.82	-20.91	-24.13	1,6

TABLE 4 - Continued

Galaxy (1)	CO (2)	$(U-V)_{0.5}$ (3)	$(V-K)_{0.5}$ (4)	$(J-K)_{0.5}$ (5)	$(H-K)_{0.5}$ (6)	$K_{0.5}$ (7)	$V_{1.0}$ (8)	$M_{V_{1.0}}$ (9)	$M_{K_{1.0}}$ (10)	Notes (11)
		Values at A/D(0) = 0.5					Values at A/D(0) = 1.0			
NGC 4464	0.145	1.41	3.09	0.86	0.16	9.91	12.79	-18.94	-22.24	
4472	0.17	1.64	3.38	0.90	0.19	6.12	8.89	-22.84	-26.03	
4478	0.14	1.28	3.28	0.83	0.20	8.80	11.67	-20.06	-23.35	1
4486	0.17	1.55	3.39	0.88	0.19	6.45	9.27	-22.46	-25.70	1
4486A	0.115	--	--	--	--	--	--	--	--	3
4486B	0.10	1.62	3.6	0.88	0.17	10.49	13.66	-18.07	-21.66	1,4
4494	0.135	1.34	3.06	0.85	0.18	7.83	10.43	-20.92	-23.94	1,2,6
4649	0.17	1.70	3.39	0.91	0.19	6.45	9.29	-22.44	-25.70	
4889	0.17	1.57	3.31	0.92	0.23	9.29	12.08	-23.54	-26.75	
5813	0.14	1.59	3.40	0.91	0.20	8.35	11.16	-21.62	-24.85	1
5846	0.16	1.68	3.50	0.96	0.23	7.81	10.73	-22.05	-25.39	1
5866	0.15	1.41	3.47	0.98	0.28	7.37	10.32	-21.03	-24.40	
5982	0.155	1.49	3.21	0.85	0.20	8.83	11.62	-22.18	-25.39	1
6702	0.21	1.46	3.35	0.96	0.24	9.97	13.0	-22.01	-25.5	1,2,6
7619	0.17	1.73	3.49	0.90	0.20	8.80	11.70	-22.68	-26.00	
7626	0.17	1.65	3.41	0.91	0.20	9.0	11.95	-22.43	-25.8	1,2,6

NOTES:
1. Value of V[A/D(0) = 1] not from RCBG.
2. Value of K[A/D(0) = 0.5] is extrapolated using growth curve.
3. No value for D(0) available.
4. No overlap of V and K data, so use growth curves to get $(V-K)_{0.5}$.
5. Local Group: (m-M) = 24.1.
6. Value of (J-K) extrapolated using mean slope of -0.12 (only one observation).

of field galaxies. Such a comparison results in a change of $V - K$ of -0.12 ± 0.03 for a change in $A/D(0)$ from 0.1 to 1.0. This is consistent with the value in Table 3.

b) *Integrated Properties of the Galaxies*

In order to study the integrated properties of the galaxies, we assigned to each galaxy representative values of the observed quantities, corrected for reddening and redshift at a projected aperture size of $A/D(0) = 0.5$. This value was chosen as it involves the least extrapolation of the data. The adopted values are contained in Table 4, and were derived as follows: for the CO index, any radial variations are masked by the measuring errors, and a weighted average of all the CO observations for a given galaxy was formed. These are given in column (2) of Table 4. (Values at 7″.5 and 111″ were excluded from the average because they are available for only a few galaxies.) All observations of galaxies with K magnitudes which have been measured at both $A/D(0) \gtrless 0.5$ were combined into a preliminary growth curve. This curve determined ΔK between $A/D(0) = 0.25$ and 0.75 and allowed the addition of nearly all the remaining galaxies. The data are presented in Figure 2, and representative values for the growth curve are given in Table 5. Column (7) of Table 4 gives K magnitudes ($K_{0.5}$) at $A/D(0) = 0.5$ for the galaxies based on either interpolation between observed points or extrapolation via the growth curve. A similar procedure was followed to obtain $(J - K)_{0.5}$ and $(H - K)_{0.5}$. Values of $(V - K)_{0.5}$ in column (4) of Table 4 were obtained either by interpolating between the values given in Table 1 or in a few cases by extrapolating from available V and K growth curves. The values of $(U - V)_{0.5}$ were taken from the sources used for the V magnitudes or from Paper III. In a few cases it was necessary to extrapolate available $(U - V)$ measurements to $A/D(0) = 0.5$ by use of the mean slope $\Delta(U - V)/\Delta \log A/D(0) = -0.13$ (Paper III).

To obtain absolute magnitudes, we used values of $V_{1.0}$ from RCBG, with changes made when new data from the literature or Paper III were available. Mean redshifts corrected for galactic rotation are from RCBG, and a Hubble constant of 50 km s^{-1} Mpc^{-1} was adopted. For those galaxies identified as being in small groups (de Vaucouleurs 1976), the mean redshift of the group was used; all galaxies considered to be in the Virgo cluster were assigned the same redshift. For Local Group members in the vicinity of M31 and M33, with NGC 404 included, a value of $(m - M)_0 = 24.1$ was used (van den Bergh 1976). The absolute K magnitudes $M_{K_{1.0}}$ were derived from $(K_{0.5} - K_{1.0}) = 0.42$ mag (Table 5).

i) *Color-Color Relationships*

In Figures 3–5, we present the interrelationships between the CO index and the broad-band colors, and we list in Table 6 some least-squares fits to the data points. The points for the globular clusters in these figures have not been included in the least-squares solutions. These data will be discussed in § IV. Several basic results are apparent from Figures 3 and 4. (1) The location of the points in a CO index versus color diagram reiterates our previous conclusion that the light of early-type galaxies is dominated by giant stars (Frogel *et al.* 1975*a*, *b*). (2) The CO index shows no significant dependence on color for the galaxies in this sample. In fact, with a few exceptions, the observed dispersion in the CO index is consistent with that expected from the measuring errors alone. (3) The *average* broad-band colors indicate a mean spectral type which depends on wavelength. This is the same effect noted by Stebbins and Whitford (1948); viz., the light of elliptical galaxies is of a composite nature, and as the observational baseline shifts to the red, we sample, in the mean, a later and later component of the stellar population. $H - K$, the reddest color, corresponds to that of an M star. In Figure 5 we plot $V - K$ and $J - K$ against $U - V$. The $V - K$ color is

TABLE 5

Adopted K Growth Curve

Log A/D(0)	Δ Mag (K)	Log A/D(0)	Δ Mag (K)
-1.1	+1.57	-0.4	+0.16
-1.0	+1.34	-0.3	0.0
-0.9	+1.13	-0.2	-0.15
-0.8	+0.91	-0.1	-0.29
-0.7	+0.70	0.0	-0.42
-0.6	+0.50	+0.1	-0.55
-0.5	+0.33		

TABLE 6

COLOR-COLOR AND COLOR-MAGNITUDE RELATIONS OF THE FORM $Y = A + BX$

X	Y	N	$A(\pm\sigma)$	$B(\pm\sigma)$	r	s
$(U - V)_{0.5}$	$(V - K)_{0.5}$	47	1.35 (0.14)	+1.28 (0.09)	+0.89	0.11
$(U - V)_{0.5}$	$(J - K)_{0.5}$	47	0.57 (0.07)	+0.21 (0.05)	+0.65	0.04
$M_{V_{1.0}}$	$(U - V)_{0.5}$	47	0.22 (0.32)	−0.06 (0.02)	−0.73	0.11
$M_{V_{1.0}}$	$(V - K)_{0.5}$	47	1.69 (0.35)	−0.07 (0.02)	−0.69	0.19
$M_{V_{1.0}}$	$(J - K)_{0.5}$	48	0.60 (0.32)	−0.01 (0.02)	−0.51	0.05
$M_{V_{1.0}}$	CO*	41	0.03 (0.34)	−0.006 (0.016)	−0.60	0.02

* Galaxies with $z \geq 0.012$ have been excluded from the CO solution; s is the variance of the fit. The assumed uncertainties in the quantities are ±0.03, ±0.10, ±0.04, ±0.02, and ±0.2 mag for $(U - V)$, $(V - K)$, $(J - K)$, CO, and $M_{V_{1.0}}$, respectively.

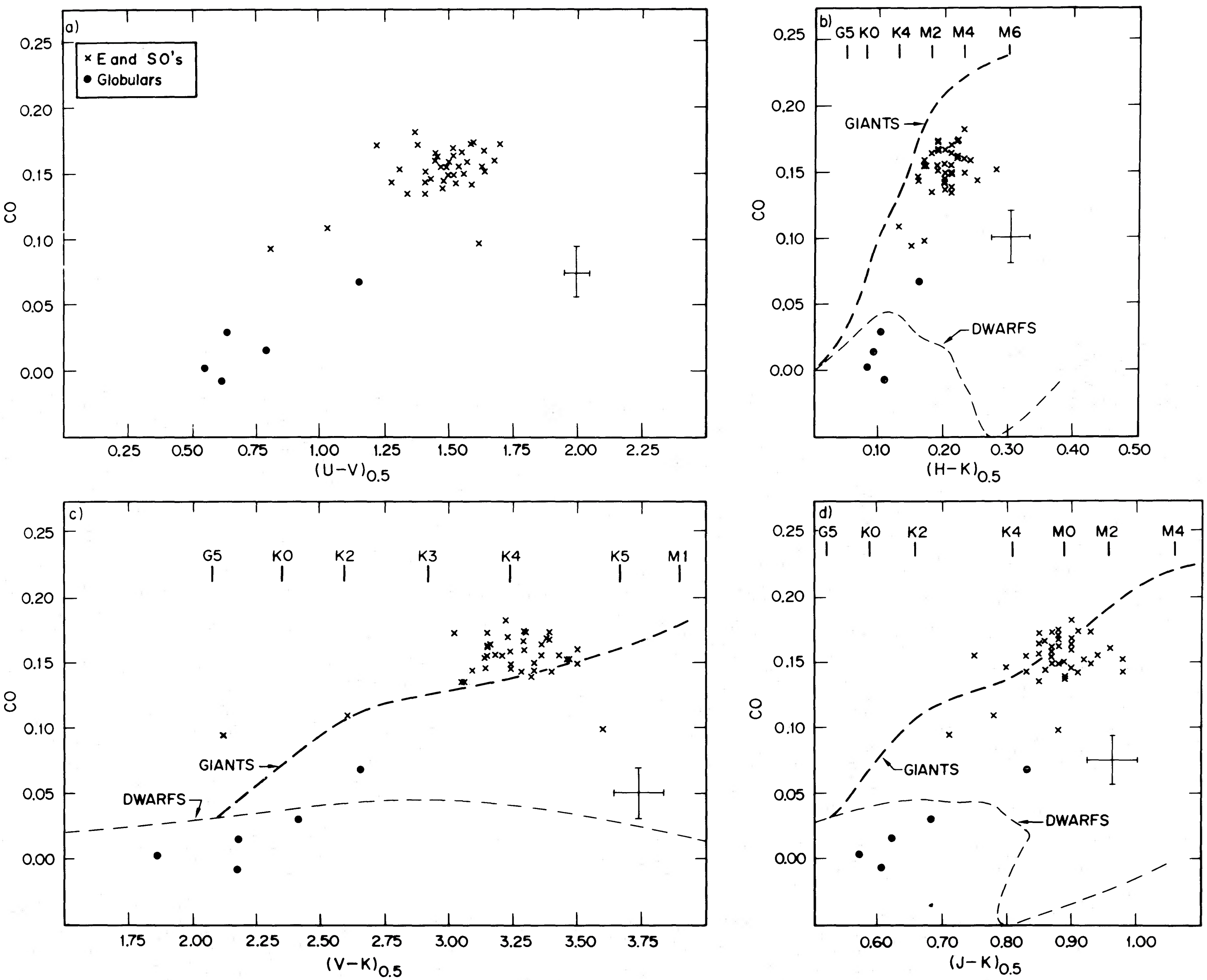

FIG. 3.—The average CO index for a galaxy as a function of several colors determined at a characteristic value of $A/D(0) = 0.5$. All the data points from Table 4 are plotted. *Dashed lines*, mean relationships for field giants and dwarfs from the Appendix. *Circles*, globular-cluster observations from Table 2. The indicated spectral types refer to the mean giant relationship.

TABLE 7

Galaxies in Clusters and de Vaucouleurs' Groups with Well-determined Distances

$M_{V_{1.0}}$	No.	Mean Colors $(U-V)_{0.5}$	$(V-J)_{0.5}$	$(V-K)_{0.5}$	$(J-H)_{0.5}$	$(H-K)_{0.5}$	CO*
$M_V < -22.8$	3	1.57	2.44	3.36	0.70	0.22	--
$-22.8 \le M_V < -21.8$	13	1.58	2.43	3.33	0.69	0.21	0.16
$-21.8 \le M_V < -20.8$	10	1.50	2.40	3.30	0.68	0.22	0.15
$-20.8 \le M_V < -19.8$	8	1.43	2.36	3.22	0.67	0.20	0.16
$-19.8 \le M_V < -18.8$	3	1.39	2.27	3.15	0.68	0.20	0.14

*Galaxies with $z \ge 0.012$ were excluded from the average CO values.

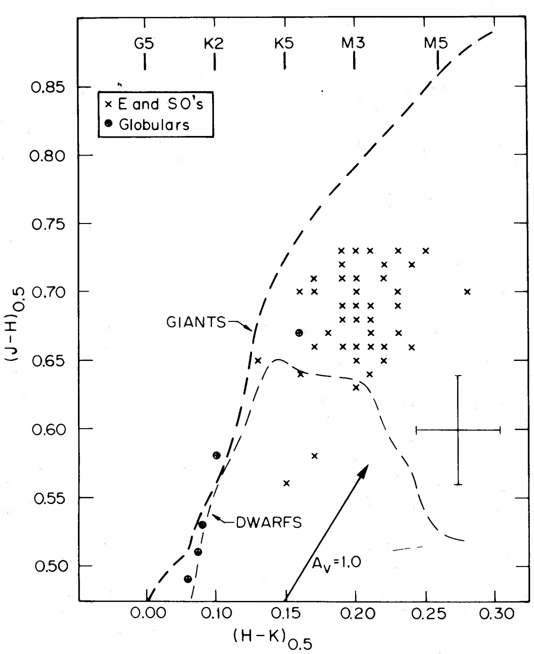

FIG. 4.—The $J - H$, $H - K$ relation for the data from Table 4. The symbols are the same as in Fig. 3.

strongly correlated with $U - V$, in agreement with the results of Strom *et al.* (1976). These correlations are discussed further below.

ii) *Color–Absolute Magnitude Relationships*

Figure 6 displays the colors and the CO index as functions of absolute magnitude; the least-squares solutions from Table 6 are also shown. That a strong correlation exists between $U - V$ and $M_{V_{1.0}}$ is well known (e.g., de Vaucouleurs 1961). The value for the slope agrees with that found from the data of Sandage (1972). As expected from Figure 5, $V - K$ also correlates with $M_{V_{1.0}}$. The extinction vectors suggest that part of the scatter in Figure 6 could arise from uncertainties in the reddening. Any significant dependence of CO index on luminosity is not established by the present data.

In order to reduce the scatter in the color–absolute magnitude relationships, the observations of galaxies with well-determined distances (i.e., those in groups or clusters) were binned in unit absolute magnitude intervals (Table 7). This table shows evidence that the $V - K$ color of the brightest galaxies is relatively independent of luminosity compared with the fainter groups. A relative flattening in color-magnitude plots was first noted by Lasker (1970); this point is discussed further in § VI*a* and in later papers in this series.

iii) *Ratios of Color Variations*

An interesting result is found when changes in the colors within galaxies are compared with changes from galaxy to galaxy. Within individual galaxies, the average change in $U - V$ is given by $\Delta(U - V)/\Delta \log A/D(0) = -0.13 \pm 0.02$, a result which is based on the measurements of Paper III and which agrees with that of Sandage (1976). We now combine this with the results of Tables 3 and 6 to arrive at the values shown in Table 8. Taken at face value, these results show that if the 0.5–2.2 μm spectral region is divided in two, then radial changes of the stellar population (owing to luminosity function and/or metallicity changes) within galaxies are most evident at wavelengths *longward* of 1.2 μm. On the other hand, from one galaxy to another such changes are evident primarily at wavelengths *shortward* of 1.2 μm.

The measurements made with the J filter were subject to the largest corrections, owing to the beam profile effects noted in § II*c*. Since the average value of $\Delta \log A/D(0)$ for the determination of $\Delta(J - K)/\Delta \log A/D(0)$ is 0.6, any residual systematic error in the $J - K$ color will be doubled. As an example, a systematic error of 0.02 mag would change $\Delta(J - K)/\Delta(U - V)$ within galaxies by nearly 0.3. Another potential difficulty with the interpretation of these numbers is that the slope *within* galaxies is determined mainly from observations of the brighter galaxies, whereas the determination of the slopes

TABLE 8

RATIOS OF COLOR VARIATIONS

Color Ratio	Within Galaxies	Between Galaxies
$\Delta(V - K)/\Delta(U - V)$	0.9 ± 0.5	1.3 ± 0.1
$\Delta(J - K)/\Delta(U - V)$	0.9 ± 0.4	0.2 ± 0.1
$\Delta(V - J)/\Delta(U - V)$	0.0 ± 0.5	1.1 ± 0.2

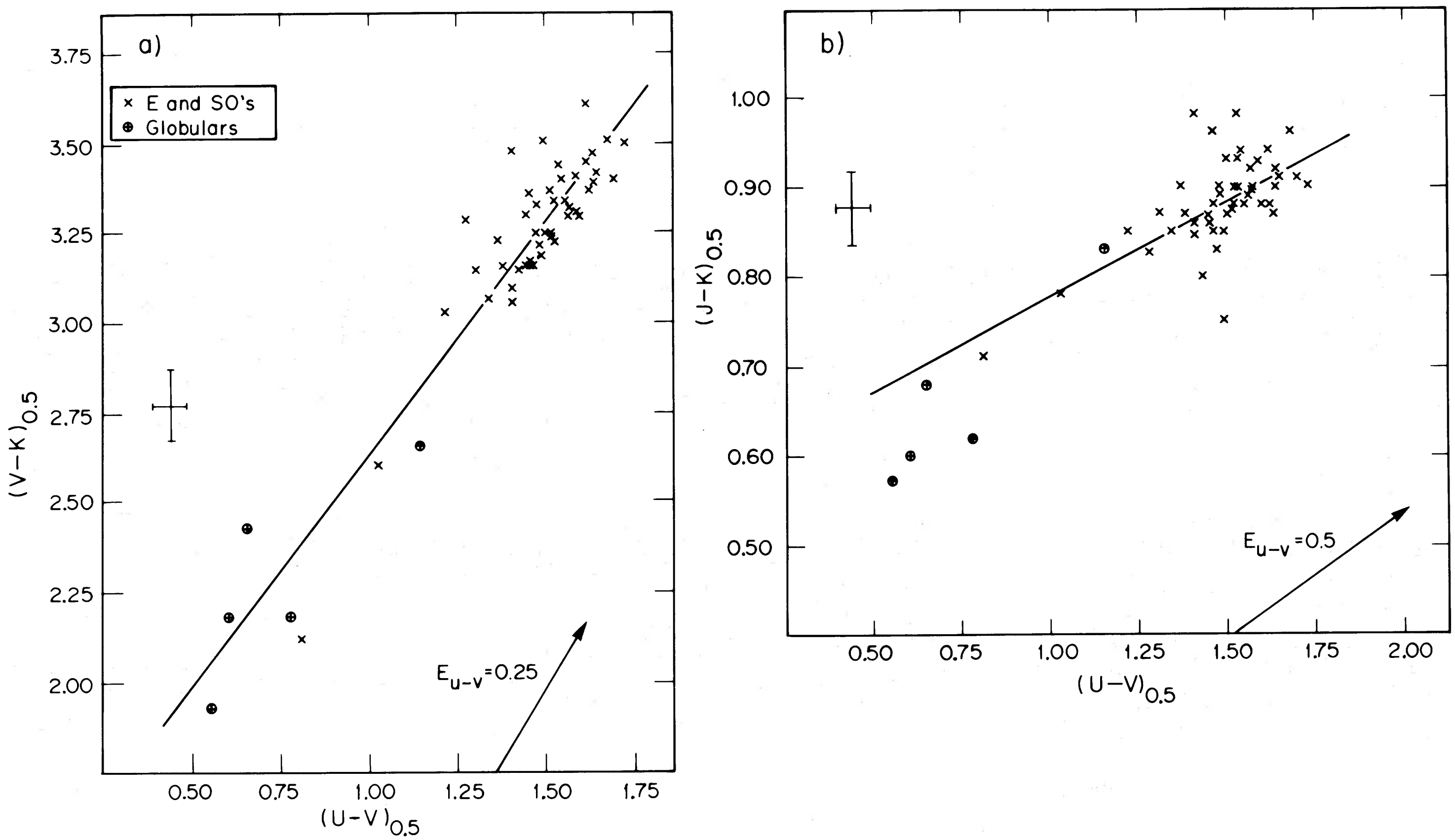

FIG. 5.—All the galaxies from Table 4 are plotted. *Open symbols*, globular-cluster data from Table 2. *Solid lines*, linear least-squares fits to the galaxy data only.

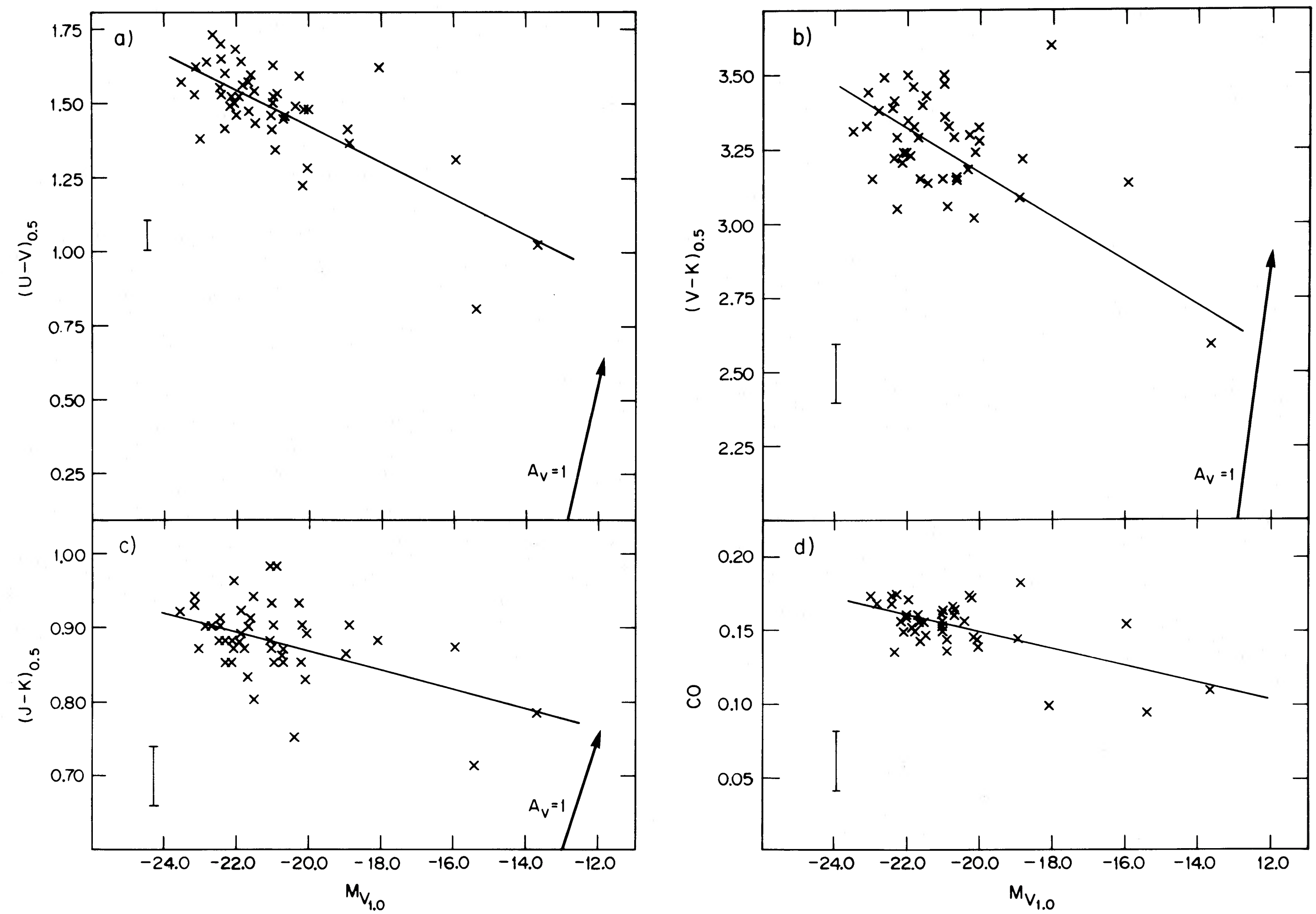

FIG. 6.—Corrected colors and CO indices for all galaxies from Table 4 are shown as functions of absolute magnitude. The linear least-squares fits are also indicated.

between galaxies is weighted toward the few galaxies of lower luminosity.

A proper resolution of the question of the color-color relationships within galaxies and between galaxies awaits detailed off-axis photometry, free of systematic beam profile effects.

c) *Summary and Conclusions*

The results presented above can be summarized as follows:

1. In combination with the reddest broad-band colors, the CO data show that the infrared light of the inner regions of early-type galaxies is dominated by the light of M giant stars.
2. The strength of the CO absorption remains constant out to a projected aperture diameter $A/D(0) = 1$. A significant dependence of CO index on absolute magnitude is not established by the data.
3. The observed dispersion in the *UVJHK* colors is due, in part, to a dependence of the colors both on the fraction of the galaxy being measured and on the galaxian luminosity. The sense of the dependences is for the colors to be redder near the nucleus and in galaxies of higher luminosity.
4. There is evidence that there are differences in the ratios of color variations between galaxies and within galaxies.

It should be noted that the above conclusions are based on data from a sample of galaxies which have a limited range in luminosity. Furthermore, averages have been taken over a sample which is inhomogeneous in several respects: a number of S0 galaxies, several local group dwarfs, and two possibly tidally stripped objects, NGC 221 and 4486B (Faber 1973*a*) have been included, and the galaxies are members of both rich and sparse groups. However, none of the correlations presented above are changed in a statistically significant way when various subsets of the data are excluded from the solutions. These points are explored in detail in future papers, where a larger sample of galaxies is studied.

IV. DISCUSSION OF THE GLOBULAR-CLUSTER OBSERVATIONS

Our preliminary study of globular clusters is based on the integrated-light data presented in Table 2. The colors are compared with those of the galaxies in Figures 3–5. M15 and M92 are examples of stellar systems with extreme metal deficiencies, M3 and M13 of moderate metal deficiencies, and M69 of only a small metal deficiency (Sandage 1970; Hartwick and Sandage 1968, and references therein). It is apparent from the color-color plots (Figs. 4 and 5) that these five clusters extend the sequences defined by the E and S0 galaxies and, in fact, overlap the two faintest galaxies NGC 205 and 404. This behavior is similar to that found from studies of optical colors and indices (e.g., McClure and van den Bergh 1968; Faber 1973*b*). Furthermore, *the ordering of these clusters by their infrared colors corresponds approximately to an ordering by metallicity in the sense that redder colors are associated with higher* (Fe/H).[4] This result differs from the finding of Grasdalen (1974), who derived $V - K$ colors for a number of highly reddened distant clusters.

The location of the clusters relative to the galaxies on plots of CO versus color (Fig. 3) may differ from the relative locations on color-color plots. There is evidence that, for a given color, the CO strengths in globular clusters are weaker than would be estimated from a linear extrapolation of the available galaxy data. Alternatively, it is possible that the CO index for galaxies turns sharply downward below $V - K = 3.0$.

V. COMPARISON OF MEAN COLORS WITH STELLAR SYNTHESIS MODELS

Recently, attempts have been made by several authors (Tinsley and Gunn 1976; O'Connell 1976*b*; Whitford 1977) to model photometric and spectrophotometric observations of the central regions of bright elliptical galaxies. In this section, we ask how well these published models agree with our new data for bright galaxies. Detailed model fitting is deferred to a later paper.

Two models are chosen as examples: Model A of Tinsley and Gunn (1976, TG), in which the slope of the initial mass function x equals zero; and model C of O'Connell (1976*b*, OC) with a flat luminosity function φ (M dwarfs), which corresponds to an x of about 0.5. The published luminosity function of TG and unpublished values from O'Connell (1976*c*) were combined with the stellar calibrations of the Appendix and of Johnson (1966*b*), and the colors for these two models were calculated. (Johnson's $J - K$ colors were transformed to the system of this paper as discussed in the Appendix.) The results are given in Table 9, where the observed values are for the galaxies in the second group of Table 7. The OC model gives an excellent fit to the average galaxy colors, while the TG model has colors which are too blue and a CO index which is too weak. OC's model fit is probably fortuitous, however, because of the sensitivity of the infrared indices to the luminosity function of the giant branch (see Table 12), combined with the coarseness of OC's bins for giants. The origin of the difference between the two models lies in the choice of the relative shape of the giant

[4] Observations of individual stars in clusters (Cohen, Frogel, and Persson 1978) in fact show that, for a constant effective temperature, the CO index decreases with decreasing metallicity.

TABLE 9

COMPARISON BETWEEN MODELS AND OBSERVATIONS

Parameter	TG	OC	Obs.
$V - K$	2.97	3.29	3.33
$J - H$	0.59	0.7	0.70
$H - K$	0.22	0.2	0.20
CO	0.14	0.16	0.16
M/L_V	3.0	2.4	...

branch luminosity function, and in the assumed values of M_V for giants (which differed by up to 1 mag). For the OC model, about 35% of the light at 2 μm comes from the M6 III bin, whereas these stars contribute only 12% of the 2 μm light in the TG model. Nevertheless, the model-fitting work of TG (and references therein), OC, and Frogel *et al.* (1975*a*) has established that *the* $V - K$ *color and the* CO *index provide strong constraints on both the dwarf-to-giant ratio and the shape of the giant branch—*$V - K$ *is effective for the latter and the* CO *index for the former*. Any significant increase in the number of late-type dwarf stars beyond those already contained in the models drives the CO index to unacceptably low values and begins to make $V - K$ too red. The $J - H$ color is mildly sensitive to the giant-to-dwarf ratio, since dwarf stars do not exhibit $J - H$ colors greater than 0.7 (see, e.g., Mould and Hyland 1976). $H - K$ provides a weak constraint on the giant branch luminosity function, as can be seen from Figure 4: stars later than M3 III must be present to provide the red $H - K$ color.

VI. COMPARISON WITH PHOTOMETRIC STUDIES AT $\lambda < 1.0\ \mu$m

In this section we compare our results with those of three previous photometric studies of the nuclei of early-type galaxies and of the integrated light of globular clusters—O'Connell (1976*a*), Faber (1973*b*), and McClure and van den Bergh (1968).

a) *The Work of O'Connell*

Nineteen E and S0 galaxies were observed photoelectrically by O'Connell (1976*a*) in the extreme red region of the optical spectrum, mostly through a 12″ diameter aperture. The results of immediate interest here may be summarized as follows: A $(1.0 - 0.74)_0$ color, which is insensitive to blanketing effects, shows a "mild color-luminosity dependence" over the range $-22 < M_V < -16$. However, if the faintest galaxies are excluded, then O'Connell's data are consistent with a constant $(1.0 - 0.74)_0$ color for $M_V < -19$. This color is "equivalent to an M0–1 III star." O'Connell also found that the strength of the Ca II + TiO λ8542 feature (which is positively correlated with luminosity in giant stars), rather than increasing monotonically with absolute galaxian magnitude, reaches a maximum near $M_V = -20$, and then declines with increasing luminosity. He interprets this as a decrease in the luminosity of the late M giants in the brightest galaxies owing to the increased metal content of these systems.

All but one of O'Connell's galaxies were observed by us through either a 15″ or a 16″.5 diameter aperture. These observations were taken from Table 1 and divided into the three luminosity groups used by O'Connell. The colors and CO index showed no statistically significant variation from group to group. These results did not change when other galaxies with 15″ or 16″.5 observations from Table 1, and having reliable distance estimates, were included in the averaging.

To carry this comparison further, we use the averaged colors from Table 7. Although these measurements refer to a much larger fraction of the light than that measured by O'Connell, these data are expected to have smaller uncertainties than the small-aperture data, and they substantially increase the sample size. From the decrease in Ca II + TiO strength for $M_V < -20$, one might expect to see some effect in the infrared colors, especially in $V - K$. Table 7 shows no evidence that any of the colors become bluer with increasing luminosity. A much larger sample of galaxies is needed to proceed further with this puzzling comparison.

b) *The Work of McClure and van den Bergh and of Faber*

McClure and van den Bergh (1968) and Faber (1973*b*) observed the central regions of a number of E/S0 galaxies and the integrated light of globular clusters with sets of narrow bandpass filters chosen to isolate specific spectral features primarily in the blue and visible. The UV blanketing feature measured by McClure and van den Bergh (1968) (defined by them as C*[38–45]) was found to be strongly correlated with *Q*, the reddening-free metallicity index. On the basis of these results and of model fitting, they concluded that dwarf ellipticals consist primarily of metal-deficient stars, that the cores of giant ellipticals consist of metal-rich stars with strong CN bands, and that these cores are embedded in a metal-poor halo. Additional evidence that a stellar population with strong CN bands is present in the nuclei of galaxies has been presented by McClure (1969), Spinrad *et al.* (1971), Welch and Forrester (1972), and Spinrad, Smith, and Taylor (1972), among others.

Faber's (1973*b*) observations of galaxies and globular clusters led her to the following conclusions: (*a*) all of the colors depend on only one parameter—the luminosity of the galaxy; (*b*) the scatter in the data at a given M_V comes mostly from residual reddening errors and from observational errors; and (*c*) a monotonic increase in mean metallicity with luminosity seemed the most likely explanation for the observed variation in the various indices.

In Figure 7 we compare the values of $(U - V)_{0.5}$, $(V - K)_{0.5}$, $(J - K)_{0.5}$, and CO for the galaxies and the globular clusters from Tables 2 and 5 with the $CN_0 - Mg_0$ line index of Faber (1973*b*). Some of the measurements of McClure and van den Bergh were transformed to the $CN_0 - Mg_0$ index via a comparison of objects in common and were added to Figure 7. The correlations seen in Figure 7 are in qualitative agreement with those expected from the relations between Faber's line index and absolute magnitude and from our own results in Figure 6, in that the colors and CO index are seen to increase monotonically with increasing $CN_0 - Mg_0$. A slight curvature may be present in Figure 7*c*, and this could be another indication that there is a relative insensitivity of the infrared colors of brighter galaxies to changes in M_V. Aside from this latter point, though, the data in Figures 5, 6,

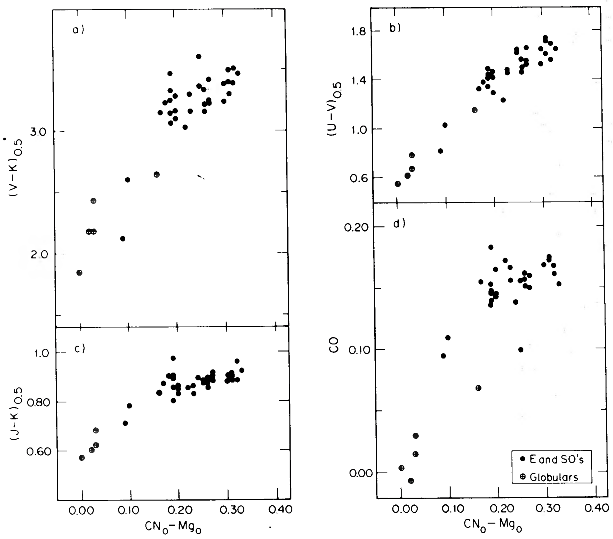

FIG. 7.—Colors and CO indices for galaxies from Table 4 and for globular clusters from Table 2 are shown as functions of Faber's (1973*b*) $CN_0 - Mg_0$ index.

and 7 are in basic agreement with Faber's (1973*b*) main conclusions.

VII. SUMMARY AND CONCLUSIONS

In this paper we have presented new broad-band infrared colors and CO indices for early-type galaxies and globular clusters. We have compared our data with recent stellar synthesis models of bright ellipticals and conclude that the only models which are consistent with the present observations are those with rich giant branches and relatively flat main-sequence luminosity functions. A detailed quantitative comparison is made difficult, however, by the sensitivity of the predicted infrared colors to the numbers and luminosities of M giants, combined with the observational uncertainties in these latter quantities.

We have examined the dependence of the various colors on absolute galaxian luminosity and on measuring aperture size. The broad-band colors tend to redden with increasing luminosity and with decreasing aperture size. Since we find evidence that the infrared colors and the CO index are redder and stronger, respectively, in globular clusters of high mean metallicity as opposed to those of low metallicity, it is reasonable to conclude that the changes observed in the integrated light of galaxies also have, as their underlying cause, changes in the mean metallicity of the stellar population. A change in the metallicity acts both directly via a change in the CO strength for stars of the same effective temperature and indirectly via a change in the relative populations of the principal sequences of a color-magnitude diagram. Of particular note is the evidence that the relative changes of the $U - V$, $V - J$, and $J - K$ colors within galaxies differ from those between galaxies. It may be possible to understand this result qualitatively if some fraction of the changes in the optical parameters arises from changes in CN blanketing rather than from changes in [Fe/H] alone (Peterson 1976*a*, *b*). This may mean that $U - V$ cannot be used as a pure indicator of the mean metallicity of a composite system. The color changes in systems consisting of metal-rich and metal-poor stars may also be important in understanding the interplay of $U - V$ and $V - K$. Stellar synthesis models of a complexity greater than any heretofore reported in the literature, and which include a certain amount of chemical evolution, will be required for the quantitative interpretation of these and other recent photometric observations of galaxies.

This program would not have been possible without the generous allotment of observing time made available to us, particularly at the Hale Observatories, or without the collaboration of Eric Becklin and Gerry Neugebauer. We are grateful to Allan Sandage for allowing us to have access to his compilation of published optical photometry and for his continued interest in this work. We acknowledge helpful conversations with Beatrice Tinsley and Robert O'Connell. Special assistance was provided by J. Walker and G. Livet. An anonymous referee made several critical comments on an earlier version of this paper. This work was supported in part by NSF grant AST 74-18555 A2 and NASA grant NGL 05-002-207.

APPENDIX

Although the J and K filters used in this study are similar to those employed in the original infrared photometric system as described by H. L. Johnson and others, the need for a high degree of internal accuracy necessitated the determination of a new set of standard magnitudes. Twenty-one stars, selected so that a reasonably large range of brightness and color could be spanned, were set up as standards.

Individual standards were typically observed on 10–20 different nights with between one and three observations per night. The system was closed once around the sky, and no systematic closure errors were found. We estimate that the *internal* accuracy of the system is ± 0.01 mag at H and K and in the CO index, and ± 0.03 mag at J. A combination of the transmission characteristics of the J filter, the atmosphere, and the field lens, and the rounded nature of the beam profile, causes the J measurements to have the largest uncertainty.

Table 10 contains the $J - H$ and $H - K$ colors, K magnitudes, and CO indices for our grid of standards. The zero point of this system is set by defining the magnitudes and colors of α Lyr to be 0.00 at all wavelengths. If allowance is made for the fact that Johnson (1966*b*, and references therein) takes $K(\alpha \text{ Lyr}) = +0.02$, there is no systematic difference between the magnitude scales of Johnson and of Table 10 based on a comparison of 16 stars. Thus, except for the zero-

TABLE 10

STANDARD STARS

Name	Sp. Type	V	K	J-H	H-K	CO
BS 117	M0 III	5.71	1.87	0.74	0.16	0.155
BS 134	K0 III	6.30	4.07	0.45	0.08	0.04
BS 718	B9 III	4.28	4.38	-0.05	-0.02	0.00
BS 923	K0 III	5.99	3.74	0.49	0.08	0.05
BS 1552	B2 III	3.69	4.14	-0.04	-0.05	0.00
BS 1698	K3 III	4.46	1.84	0.53	0.10	0.095
BS 3304	K5 III	5.63	2.37	0.66	0.13	0.15
BS 3403	K2 III	4.59	1.88	0.54	0.06	0.08
BS 3427	K0 III	6.39	4.25	0.48	0.07	0.04
BS 4039	dF5	5.82	4.49	0.28	0.03	-0.005
BS 4550	G8 VI	6.45	4.42	0.44	0.06	0.005
BS 4608	G8 III	4.13	1.89	0.47	0.05	0.05
BS 4689	A2 V	3.88	3.77	-0.05	-0.01	-0.005
HD 107906	K	--	7.04	0.39	0.05	0.035
HD 132950	K	--	6.33	0.51	0.07	0.04
BS 5634	F5 V	4.92	3.88	0.22	0.02	0.00
BS 6092	B5 IV	3.89	4.30	-0.06	-0.05	0.01
BS 6136	K4 III	5.39	2.02	0.66	0.14	0.145
BS 6228	K5 III	5.16	1.44	0.72	0.15	0.165
BS 7001	A0 V	0.00	0.00	0.00	0.00	0.00
BS 8498	K3 II-III	4.12	0.99	0.62	0.13	0.15
BS 8551	K0 III-IV	4.80	2.29	0.53	0.09	0.07

TABLE 11

SELECTED M GIANTS AND SUPERGIANTS

Name	Sp. Type	K	J-H	H-K	CO
BS 3027	M2 II-III	2.01	0.83	0.20	0.20
BS 3705	M0 III	-0.61	0.84	0.16	0.17
BS 4008	M0 III	2.10	0.80	0.17	0.20
BS 4069	M0 III	-0.84	0.79	0.15	0.18
BS 4336	M2 III	1.44	0.79	0.18	0.20
BS 4902	M3 III	0.14	0.82	0.20	0.20
BS 4910	M3 III	-1.25	0.80	0.18	0.21
BS 5879	gM1	0.05	0.82	0.17	0.19
BS 7139	M4 II	-1.17	0.85	0.21	0.26
BS 7157	M5 III	-2.06	0.83	0.26	0.25
BK Vir	M7 III	-0.91	0.89	0.33	0.25
SW Vir	M7 III	-1.88	0.91	0.34	0.27
RT Vir	M8 III	-1.18	0.90	0.36	0.24
BC Cyg	M4 Ia	0.25	1.17	0.54	0.33
AZ Cyg	M2 Ia	1.31	0.97	0.38	0.34
KY Cyg	M4 Ia	1.54	1.27	0.59	0.30
+9° 3920	M2 III	4.37	0.85	0.22	0.21
+29° 3730	M4 III	1.95	0.85	0.24	0.21
+35° 4138	M3 III	3.89	0.86	0.23	0.20
+59° 2541	M2.5 III	4.46	0.85	0.26	0.18
+64° 1842	M2 II	3.11	1.03	0.33	0.19
+42° 1065	M0 III	5.66	0.83	0.20	0.14

point shift, the $V - K$ values in this paper are on the system of Johnson. Because the effective wavelength of our J filter is different from that of Johnson, a small transformation exists between the two systems. To transform the J magnitudes of this paper to the Johnson (1966*b*) system, the following equation is adequate:

$$J_J = 1.09(J - H) + H, \qquad \text{(A1)}$$

i.e., the $J - K$ colors in this paper are systematically blue compared with Johnson's. We caution other observers using the photometric system defined by these stars to check carefully for the presence of a color equation, particularly at 1.2 μm.

Table 11 contains measurements of selected high-luminosity late-type stars. These data were used to define mean relationships among colors, CO index, and spectral type, and can be employed to establish transformations from the present photometric system to any other system. The three supergiants in Cygnus, plus the stars identified with BD numbers, are heavily reddened (Lee 1970).

Table 12 gives the adopted mean relationships based on the system of Tables 10 and 11. The $V - K$ and $J - K$ colors as functions of spectral type for the giants are transformed from Johnson (1966*b*) for stars earlier than M0 and from Lee (1970) for M0–M6. The $H - K$ colors and CO indices of the giants are from the data of Tables 10 and 11 and from additional unpublished measurements. All of the mean values for the dwarfs are based on our own infrared measurements plus V magnitudes from the literature. The agreement with most of the recently published infrared photometry of dwarfs (e.g., Mould and Hyland 1976) is generally better than ± 0.02 mag at all wavelengths. Our observations of late-type dwarfs are discussed by Persson, Aaronson, and Frogel (1977).

TABLE 12

ADOPTED MEAN COLORS

	Giants				Dwarfs			
Sp. Type	V-K	J-H	H-K	CO	V-K	J-H	H-K	CO
G5	2.08	0.47	0.05	0.03	1.25	0.26	0.04	0.01
G8	2.16	0.49	0.06	0.04	1.50	0.32	0.05	0.02
K0	2.35	0.51	0.08	0.07	1.75	0.37	0.06	0.02
K1	2.48	0.54	0.09	0.09	2.00	0.42	0.07	0.03
K2	2.59	0.56	0.10	0.11	2.25	0.47	0.08	0.04
K3	2.92	0.62	0.12	0.12	2.50	0.52	0.09	0.04
K4	3.24	0.68	0.13	0.14	2.75	0.56	0.10	0.04
K5	3.67	0.73	0.15	0.15	3.00	0.59	0.11	0.04
M0	3.74	0.74	0.16	0.17	3.25	0.63	0.13	0.04
M1	3.90	0.76	0.17	0.18	3.50	0.65	0.14	0.04
M2	4.16	0.77	0.18	0.19	3.75	0.65	0.16	0.03
M3	4.63	0.79	0.20	0.21	4.00	0.63	0.21	0.02
M4	5.34	0.81	0.23	0.22	4.25	0.60	0.22	0.00
M5	6.20	0.86	0.26	0.23	4.50	0.57	0.24	-0.02
M6	7.20	0.89	0.30	0.24	4.75	0.54	0.25	-0.03
M7	--	0.91:	0.33:	0.25:	5.00	0.53	0.26	-0.04
M8	--	0.89:	0.37:	0.26:	5.25	0.52	0.28	-0.05
					5.50	0.53	0.29	-0.05
					5.75	0.54	0.31	-0.04
					6.00	0.55	0.32	-0.04
					6.25	0.57	0.33	-0.03
					6.50	0.59	0.35	-0.03
					6.75	0.61	0.36	-0.02
					7.00	0.62	0.37	-0.02
					7.25	0.63	0.38	-0.01
					7.50	0.65	0.39	-0.01

REFERENCES

Aaronson, M., Frogel, J. A., and Persson, S. E. 1978, *Ap. J.*, **220**, in press (Paper II).
Baldwin, J. R., Danziger, I. J., Frogel, J. A., and Persson, S. E. 1973, *Ap. Letters*, **14**, 1.
Baldwin, J. R., Frogel, J. A., and Persson, S. E. 1973, *Ap. J.*, **184**, 427.
Code, A. D. 1959, *Pub. A.S.P.*, **71**, 118.
Cohen, J. G., Frogel, J. A., and Persson, S. E. 1978, in preparation.
de Vaucouleurs, G. 1961, *Ap. J. Suppl.*, **5**, 233.
———. 1976, in *Galaxies and the Universe*, ed. A. Sandage, M. Sandage, and J. Kristian (Chicago: University of Chicago Press), p. 557.
de Vaucouleurs, G., and de Vaucouleurs, A. 1964, *Reference Catalogue of Bright Galaxies* (Austin: University of Texas Press) (RCBG).
Faber, S. M. 1972, *Astr. Ap.*, **20**, 361.
———. 1973*a*, *Ap. J.*, **179**, 423.
———. 1973*b*, *Ap. J.*, **179**, 731.
Frogel, J. A. 1971, Ph.D. thesis, California Institute of Technology.
Frogel, J. A., Persson, S. E., Aaronson, M., Becklin, E. E., and Matthews, K. 1975*a*, presented at Tercentenary Symposium, Royal Greenwich Observatory.
Frogel, J. A., Persson, S. E., Aaronson, M., Becklin, E. E., Matthews, K., and Neugebauer, G. 1975*b*, *Ap. J.* (*Letters*), **195**, L15.
———. 1975*c*, *Ap. J.* (*Letters*), **200**, L123.
Grasdalen, G. L. 1974, *A.J.*, **79**, 1047.
Hartwick, F. D. A., and Sandage, A. 1968, *Ap. J.*, **153**, 715.
Hesser, J. E., Hartwick, F. D. A., and McClure, R. D. 1976, preprint.
Johnson, H. L. 1966*a*, *Ap. J.*, **143**, 187.
———. 1966*b*, *Ann. Rev. Astr. Ap.*, **3**, 193.
———. 1966*c*, in *Nebulae and Interstellar Matter*, ed. B. M. Middlehurst and L. H. Aller (Chicago: University of Chicago Press), p. 167.
Johnson, H. L., and Méndez, M. E. 1970, *A.J.*, **75**, 785.
Kron, G. E., and Mayall, N. U. 1960, *A.J.*, **65**, 581.
Lasker, B. M. 1970, *A.J.*, **75**, 21.
Lee, T. A. 1970, *Ap. J.*, **162**, 217.
McCammon, D., Münch, G., and Neugebauer, G. 1967, *Ap. J.*, **147**, 575.
McClure, R. D. 1969, *A.J.*, **74**, 50.
McClure, R. D., and van den Bergh, S. 1968, *A.J.*, **73**, 313.
Morgan, W. W., and Mayall, N. U. 1957, *Pub. A.S.P.*, **69**, 291.
Moroz, V. I. 1966, *Soviet Astr.—AJ*, **10**, 47.
Mould, J. R., and Hyland, A. R. 1976, *Ap. J.*, **208**, 399.
O'Connell, R. W. 1974, *Ap. J.* (*Letters*), **193**, L49.
———. 1976*a*, *Ap. J.* (*Letters*), **203**, L1.
———. 1976*b*, *Ap. J.*, **206**, 370 (OC).
———. 1976*c*, private communication.
Persson, S. E., Aaronson, M., and Frogel, J. A. 1977, *A.J.*, **82**, 729.
Persson, S. E., Frogel, J. A., and Aaronson, M. 1978, in preparation (Paper III).
Peterson, C. J., and King, I. R. 1975, *A.J.*, **80**, 427.
Peterson, R. 1976*a*, *Ap. J. Suppl.*, **30**, 61.
———. 1976*b*, *Ap. J.* (*Letters*), **210**, L123.
Sandage, A. 1961, *Ap. J.*, **134**, 916.
———. 1970, *Ap. J.*, **162**, 841.
———. 1972, *Ap. J.*, **176**, 21.
———. 1973, *Ap. J.*, **183**, 711.
———. 1976, private communication.
Schild, R., and Oke, J. B. 1971, *Ap. J.*, **169**, 209.
Spinrad, H., Gunn, J. E., Taylor, B. J., McClure, R. D., and Young, J. W. 1971, *Ap. J.*, **164**, 11.
Spinrad, H., Smith, H. I., and Taylor, D. J. 1972, *Ap. J.*, **175**, 649.
Spinrad, H., and Taylor, B. J. 1971, *Ap. J. Suppl.*, **22**, 445.
Stebbins, J., and Whitford, A. E. 1948, *Ap. J.*, **108**, 413.
Strom, K. M., Strom, S. E., Jensen, E. B., Moller, J., Thompson, L. A., and Thuan, T. X. 1977, *Ap. J.*, **212**, 335.
Strom, S. E., Strom, K. M., Goad, J. W., Vrba, F. J., and Rice, W. 1976, *Ap. J.*, **204**, 684.
Tifft, W. G. 1969, *A.J.*, **74**, 354.
———. 1973, *Pub. A.S.P.*, **85**, 283.
Tinsley, B. M. 1973, *Ap. J.* (*Letters*), **184**, L41.
———. 1975, in "7th Texas Symposium on Relativistic Astrophysics," ed. P. G. Bergmann, E. J. Fenydes, and L. Mott, *Ann. NY Acad. Sci.*, **262**, 436.
Tinsley, B. M., and Gunn, J. E. 1976, *Ap. J.*, **203**, 52 (TG).
van den Bergh, S. 1967, *A.J.*, **72**, 70.
———. 1976, in *Galaxies and the Universe*, ed. A. Sandage, M. Sandage, and J. Kristian (Chicago: University of Chicago Press), p. 509.
Welch, G. A., and Forrester, W. T. 1972, *A.J.*, **77**, 333.
Whitford, A. E. 1971, *Ap. J.*, **169**, 215.
———. 1976, in *Galaxies and the Universe*, ed. A. Sandage, M. Sandage, and J. Kristian (Chicago: University of Chicago Press), p. 159.
———. 1977, *Ap. J.*, **211**, 527.
Woolf, N. J., Schwarzschild, M., and Rose, W. K. 1964, *Ap. J.*, **140**, 833.

MARC AARONSON: Steward Observatory, University of Arizona, Tucson, AZ 85721

JAY A. FROGEL: Cerro Tololo Inter-American Observatory, P.O. Box 26732, Tucson, AZ 85726

K. MATTHEWS: California Institute of Technology, 1201 E. California St., Pasadena, CA 91125

S. E. PERSSON: Hale Observatories, 813 Santa Barbara St., Pasadena, CA 91101